

Supporting Information

TiO₂ Nanoparticles Functionalized with Non-Innocent Ligands Allow Oxidative Photocyanation of Amines with Visible/Near-Infrared Photons

Alexander M. Nauth,^{a,†} Eugen Schechtel,^{b,†} René Dören,^b Wolfgang Tremel,^{*,b} and Till Opatz^{*,a}

^a Institut für Organische Chemie, Johannes Gutenberg-Universität Mainz, Duesbergweg 10-14, D-55128 Mainz, Germany

^b Institut für Anorganische Chemie und Analytische Chemie, Johannes Gutenberg-Universität Mainz, Duesbergweg 10-14, D-55128 Mainz, Germany

[†]These authors contributed equally to this work.

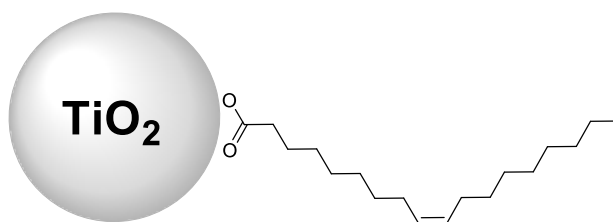
Content

1. Synthesis of TiO ₂ -DHMIQ	- S2 -
2. Nanoparticle Characterization	- S6 -
3. General Procedure & Setup	- S14 -
4. Analytical Data	- S16 -
5. Reaction Screening	- S23 -
6. Additional NMR Spectra	- S29 -
7. Mechanistic Studies	- S62 -
8. References	- S67 -

1. Synthesis of TiO₂-DHMIQ

Unless otherwise stated, all chemicals and solvents were obtained from commercial suppliers and used without further purification. Oleic acid (technical grade, 90%) was obtained from Sigma-Aldrich. Titanium(IV) *n*-butoxide (99%) was purchased from Acros Organics. Oleylamine (>50.0% (GC)) was acquired from TCI. Deionized water (18.2 MΩ·cm) was obtained from a Milli-Q water purification system (Millipore Synergy 185).

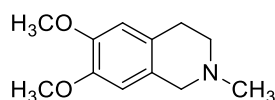
Synthesis of oleic acid-stabilized TiO₂ nanoparticles (TiO₂-OA):



Titania (TiO₂) nanoparticles (NPs) were synthesized according to a previously reported procedure.¹ Titanium(IV) butoxide (2.89 g, 2.89 mL, 8.5 mmol, 1.0 eq.) was added to a mixture of oleic acid (14.41 g, 16.24 mL, 51 mmol, 6.0 eq.), oleylamine (9.09 g, 11.19 mL, 34 mmol, 4.0 eq.) and ethanol (7.83 g, 9.93 mL, 170 mmol, 20.0 eq., absolute grade). The mixture was stirred for 15 min and transferred into a 50 mL Teflon vessel. This vessel was placed into a 250 mL Teflon-lined stainless steel autoclave, already containing 34 mL of the hydrolysis solution of ethanol and water (96:4 v/v). The sealed autoclave was then heated at 180 °C for 18 h. After opening the cooled autoclave, the content of the inner vessel was decanted into a 50 mL centrifuge tube and the crude solid product was isolated by centrifugation (9000 rpm, 10 min) and dissolved in *n*-hexane (10 mL). The white solid residue at the bottom of the inner vessel was also dissolved in *n*-hexane (10–15 mL), transferred into a 50 mL centrifuge tube and precipitated by addition of ethanol (30–35 mL, technical grade). The white precipitate was isolated by centrifugation (9000 rpm, 10 min) and redissolved in *n*-hexane (5 mL). The combined NP solutions were further purified by repeated cycles of precipitation and dissolution (3 x 30/5 mL EtOH/*n*-hexane). The last dissolution step was usually carried out in CHCl₃ (3 mL) to obtain a concentrated stock solution in a solvent that can be easily displaced for further reactions. The stock solution was stored in a tightly sealed amber glass vial with screw top, protected from sunlight, to extend its shelf life (stable solutions for at least up to a year). The exact concentration of the NP solution was determined from the remaining mass of an evaporated 100 μL aliquot (after several hours of drying at 80 °C).

¹H NMR (400 MHz, CDCl₃): δ = 5.7–5.0 (m, 2H, -CH=CH-), 2.4–0.6 (m, 31H, -CH₂- & -CH₃).

Synthesis of 6,7-dimethoxy-2-methyl-1,2,3,4-tetrahydroisoquinoline (2):



Homoveratrylamine (10.0 g, 55.2 mmol, 1.0 eq.), formic acid (16.5 g, 20.8 mL, 552 mmol, 10 eq.) and aqueous formaldehyde-solution (37 wt.%, 20.5 mL, 5.0 eq.) were combined and heated for 6 h to 100 °C. The solution was made alkaline with sodium hydroxide solution (2 M) and extracted with ethyl acetate (3 x 50 mL). The combined organic layers were dried over sodium sulfate and concentrated in vacuo to yield the crude product. After purification by column chromatography (ethyl acetate/methanol = 2:1) the product was isolated as slightly yellow solid (10.96 g, 52.87 mmol, 96%).

mp.: 75.9–78.2 °C. Lit.: 78–90 °C.²

R_f = 0.23 (ethyl acetate/methanol = 2:1).

IR (ATR): ν = 2936 (s), 2834 (m), 2768 (m), 1518 (vs), 1463 (s), 1374 (s), 1258 (vs), 1228 (vs), 1138 (vs), 1104 (s), 1013 (m) cm⁻¹.

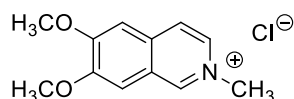
¹H NMR, COSY (300 MHz, CDCl₃): δ = 6.59 (s, 1H, H-5), 6.51 (s, 1H, H-8), 3.84 (s, 3H, OCH₃), 3.83 (s, 3H, OCH₃), 3.50 (s, 2H, H-1), 2.84 (t, ³*J*_{H-4, H-3} = 5.9 Hz, 2H, H-4), 2.66 (t, ³*J*_{H-3, H-4} = 5.9 Hz, 2H, H-3), 2.45 (s, 3H, NCH₃).

¹³C NMR, HMBC, HSQC (75 MHz, CDCl₃): δ = 147.6, 147.3 (C-6, C-7), 126.7 (C-8a), 125.8 (C-4a), 111.5 (C-5), 109.4 (C-8), 57.7 (C-1), 56.1, 56.0 (2 x OCH₃), 53.1 (C-3), 46.2 (NCH₃), 29.0 (C-4).

ESI-MS: *m/z* = 207.0 ([M+H⁺], 100%).

The spectral data match those reported in the literature.^{2,3}

Synthesis of 6,7-dimethoxy-2-methylisoquinolinium chloride (3):



6,7-Dimethoxy-2-methyl-1,2,3,4-tetrahydroisoquinoline (1.00 g, 4.83 mmol, 1.0 eq) was dissolved in acetonitrile (80 mL) and DDQ was added (2.19 g, 9.65 mmol, 2.0 eq.). The reaction mixture was refluxed and every 24 h additional DDQ (2.0 eq) was added. After 4 days and 8.0 eq. of DDQ added, LCMS indicated full conversion. The solvent was evaporated in vacuo and the solid residue was dissolved in diluted hydrochloric acid (2 M, 50 mL). The aqueous solution was extracted with diethyl ether in a Kutscher-Steudel apparatus for two days (note: ethyl acetate, chloroform or dichlormethan are not suitable in this case). The organic extract was dried over sodium sulfate and concentrated in vacuo to yield the pure iminium salt (1.04 g, 4.35 mmol, 90%).

mp.: 301–311 °C (decomposition). Lit. (iodide salt): 235–238 °C.⁴

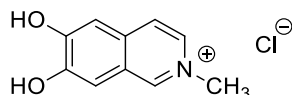
¹H NMR, COSY (300 MHz, D₂O): δ = 9.14 (s, 1H-H-1), 8.21 (dd, ³*J*_{H-3, H-4} = 6.8 Hz, ⁴*J*_{H-3, H-1} = 1.4 Hz, 1H, H-3), 8.03 (d, ³*J*_{H-4, H-3} = 6.8 Hz, 1H, H-4), 7.48 (s, 1H, H-8), 7.40 (s, 1H, H-5), 4.37 (s, 3H, NCH₃), 4.00 (s, 3H, C6-OCH₃), 3.97 (s, 3H, C7-OCH₃).

^{13}C NMR, HMBC, HSQC (75 MHz, D_2O): δ = 157.0 (C-6), 152.1 (C-7), 145.1 (C-1), 135.3 (C-4a), 133.7 (C-3), 124.0 (C-8a), 123.5 (C-4), 106.6 (C-8), 105.4 (C-5), 56.6 (C6-OCH₃), 56.2 (C7-OCH₃), 47.1 (NCH₃).

ESI-MS: m/z = 204.1 ($[\text{M}^+]$, 100%).

The spectral data match those reported in ref. 5.

Synthesis of 6,7-dihydroxy-2-methylisoquinolinium chloride (DHMIQ):



6,7-Dimethoxy-2-methylisoquinolinium chloride (890 mg, 3.71 mmol, 1.0 eq.) was dissolved in conc. hydrochloric acid (20 mL) and heated in a monomode microwave reactor (8 h, 140 °C, 20 bar, 45 W; ramp: 20 min). The solution was concentrated into dryness in vacuo to yield DHMIQ (786 mg, 3.71 mmol, quant.).

mp: 265–271 °C (decomposition).

IR (ATR): ν = 2970 (w_B), 1624 (w), 1529 (w), 1483 (m), 1436 (m), 1391 (w), 1371 (w), 1298 (s), 1173 (s), 1156 (s), 871 (s), 628 (m), 576 (m), 471 (vs) cm^{-1} .

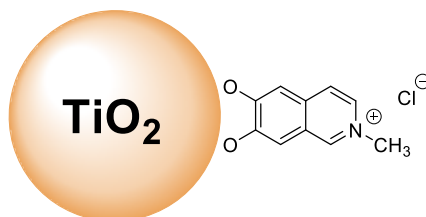
^1H NMR, COSY (300 MHz, D_2O): δ = 8.96 (s, 1H, H-1), 8.04 (dd, $^3J_{\text{H-3, H-4}}$ = 6.8 Hz, $^4J_{\text{H-3, H-1}}$ = 1.3 Hz, 1H, H-3), 7.84 (d, $^3J_{\text{H-4, H-3}}$ = 6.8 Hz, 1H, H-4), 7.30 (s, 1H, H-8), 7.18 (s, 1H, H-5), 4.30 (s, 3H, NCH₃).

^{13}C NMR, HMBC, HSQC (75 MHz, D_2O): δ = 155.2 (C-6), 149.3 (C-7), 144.7 (C-1), 134.5 (C-4a), 132.6 (C-3), 123.6 (C-8a), 122.9 (C-4), 110.5 (C-8), 108.7 (C-5), 46.9 (NCH₃).

ESI-MS: m/z = 176.0 ($[\text{M}^+]$, 100%).

ESI-HRMS: calcd for $[\text{C}_{10}\text{H}_{10}\text{NO}_2^{35}\text{Cl}]^+$: m/z = 176.0706, found: 176.0711.

Synthesis of TiO₂-DHMIQ nanoparticles:

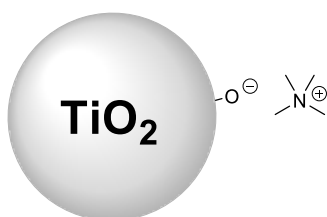


First, an aliquot of the titania stock solution, corresponding to an NP amount of 100 mg, was transferred into a 2 mL microcentrifuge tube, precipitated with excess acetone, centrifuged (14800 rpm, 3 min) and redissolved in THF (1.0 mL). The DHMIQ ligand (50 mg, 0.24 mmol) was dissolved in a ternary solvent mixture of water (1.0 mL), MeOH (0.5 mL) and THF (1.5 mL). The NP solution was added to the ligand solution, forming an opaque suspension, which was then sonicated (280 W) at 40 °C for 1 h. The reaction mixture was centrifuged (9000 rpm, 15 min), the yellow supernatant was discarded and the brownish-red pellet was dried in rough vacuum (30 mbar, 10 min). The dried NPs were redissolved in a

minimum amount of water (0.2 mL) with the aid of vortexing and sonication. After precipitation with excess THF (3.0 mL), the NPs were separated by centrifugation (9000 rpm, 10 min) and dried in rough vacuum. The DHMIQ-functionalized TiO₂ NPs were further purified by repeated cycles of dissolution, precipitation and drying as described above (6 iterations in total). To obtain an ¹H NMR spectrum of the DHMIQ-functionalized TiO₂ NPs that is not obscured by large residual signals of the undeuterated solvents, the penultimate dissolution step was performed in D₂O, followed by the ultimate precipitation step with acetone-*d*₆ and redissolution of the dried NPs in D₂O.

¹H NMR (400 MHz, D₂O): δ = 9.4–5.2 (m, 5H, Ar-H), 5.2–2.5 (m, 3H, NCH₃).

Synthesis of ligand-stripped TiO₂ nanoparticles (TiO₂-TMA):



First, an aliquot of the titania stock solution, corresponding to a NP amount of 200 mg, was precipitated with excess acetone, centrifuged (14800 rpm, 3 min) and redissolved in THF (1.0 mL). Tetramethylammonium hydroxide pentahydrate (TMAH·5H₂O, 1.0 g, 5.5 mmol) was dissolved in 1.0 mL H₂O and added to the NP solution. The combined solution was shaken and sonicated (280 W) at 40 °C for 1 h to afford a biphasic clear mixture. Addition of MeOH (2.0 mL) caused the phases to merge and the NPs were then precipitated with excess THF (15 mL). The mixture was centrifuged (9000 rpm, 10 min), the yellow supernatant was discarded and the whitish pellet was dried in rough vacuum (30 mbar, 10 min). The dried NPs were redissolved in a minimum amount of water (0.2 mL) with the aid of vortexing and sonication. After precipitation with excess THF (3.0 mL), the NPs were again separated by centrifugation (9000 rpm, 10 min) and dried in rough vacuum. The ligand-stripped TiO₂-TMA NPs were further purified by repeated cycles of dissolution, precipitation and drying as described above (4 iterations in total). To obtain an ¹H NMR spectrum of the TiO₂-TMA NPs that is not obscured by large residual signals of the undeuterated solvents, the penultimate dissolution step was performed in D₂O, followed by the ultimate precipitation step with acetone-*d*₆ and redissolution of the dried NPs in D₂O.

¹H NMR (400 MHz, D₂O): δ = 3.6–2.8 (s, 12H, N(CH₃)₄).

2. Nanoparticle Characterization

Instrumentation

Transmission electron microscopy (TEM). Samples for TEM were prepared by placing a drop of dilute NP solution in chloroform (TiO₂-OA) or water (TiO₂-DHMIQ) on a carbon-coated copper grid. TEM images for the size and morphology characterization were obtained with a FEI Tecnai 12 TWIN LaB₆ at 120 kV together with a Gatan US1000 CCD-camera (16-bit, 2048 x 2048 pixels) using the Gatan Digital Micrograph software. Size evaluation of individual nanoparticles on the TEM images was performed with ImageJ.

X-ray diffraction (XRD). X-ray diffraction patterns were recorded on a STOE Stadi P diffractometer equipped with a Dectris Mythen 1k detector in transmission mode using Mo K α_1 radiation. Crystalline phases were identified according to the Crystallography Open Database (COD) using the Match! software from Crystal Impact.

Thermogravimetric analysis (TGA). TGA analysis was performed on a Perkin Elmer Pyris 6 TGA instrument under nitrogen atmosphere (20 mL/min). A typical heat program was (i) 10 min at 30 °C, (ii) ramp of 10 °C/min from 30 °C to 600 °C and (iii) 30 min at 600 °C.

Nuclear magnetic resonance (NMR) spectroscopy. All NMR spectra were recorded at 295 K on a Bruker Avance DRX 400, a Bruker Avance III HD 300 NMR or a Bruker Avance II 400 spectrometer (Bruker Biospin GmbH, Rheinstetten, Germany).

UV/VIS absorption. UV-Vis spectra of NP dispersions in water were recorded on a Cary 5G UV-vis-NIR spectrophotometer in the range from 300 to 800 nm.

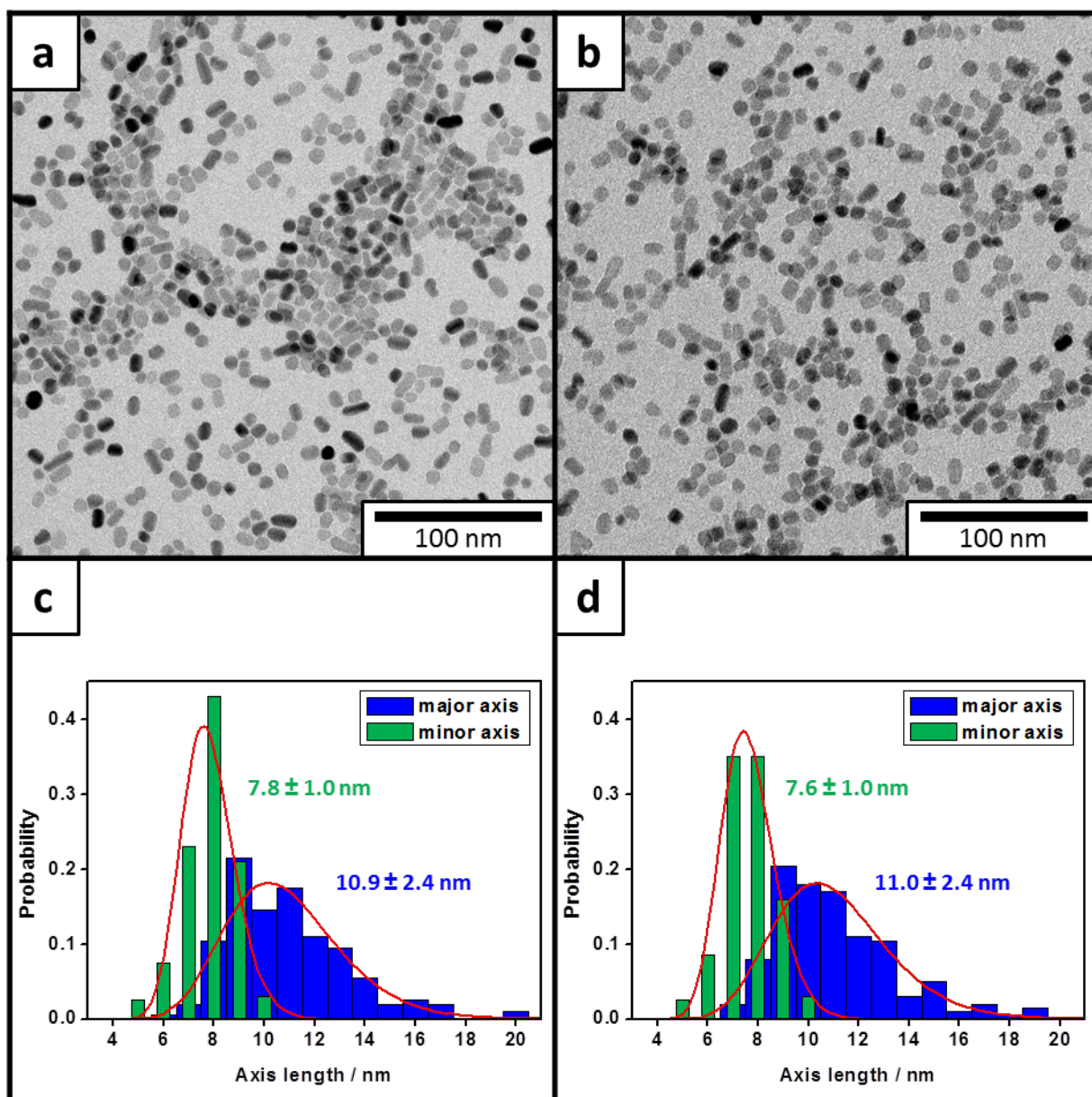


Figure S1. Transmission electron microscopic images (upper panel) and size distributions (lower panel) of (a, c) as-synthesized oleic acid-stabilized TiO₂ NPs and (b, d) DHMIQ-functionalized TiO₂ NPs. Due to their elongated shape, the NPs were fitted as ellipses with major and minor axes. Size evaluations were performed on 200 single particles before (a, c) and after (b, d) refunctionalization with DHMIQ, respectively. Surface modification with DHMIQ did not cause any changes in size or shape of the NPs.

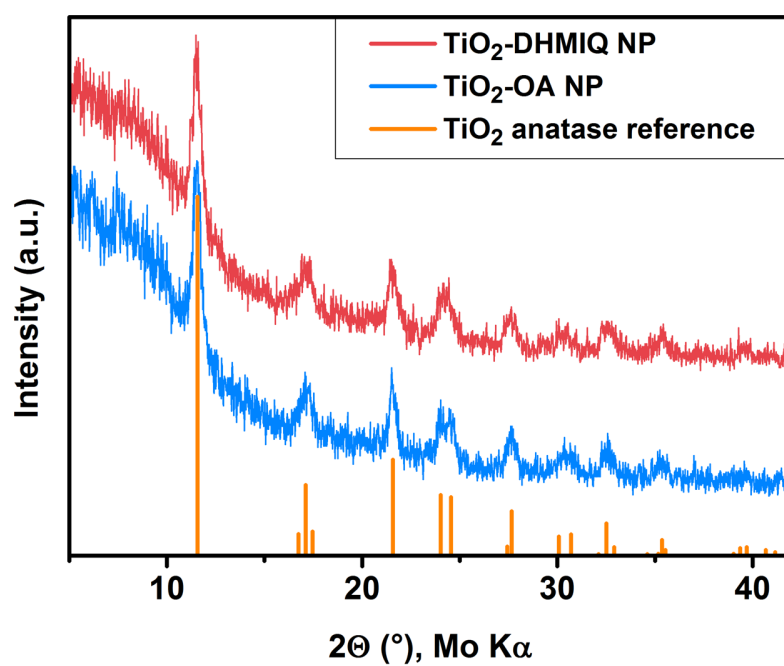


Figure S2. Powder X-ray diffractograms of TiO₂ nanoparticles before (blue curve, TiO₂-OA NP) and after DHMIQ modification (red curve, TiO₂-DHMIQ NP), both matching the bulk anatase TiO₂ reference pattern (in orange, COD 96-500-0224).

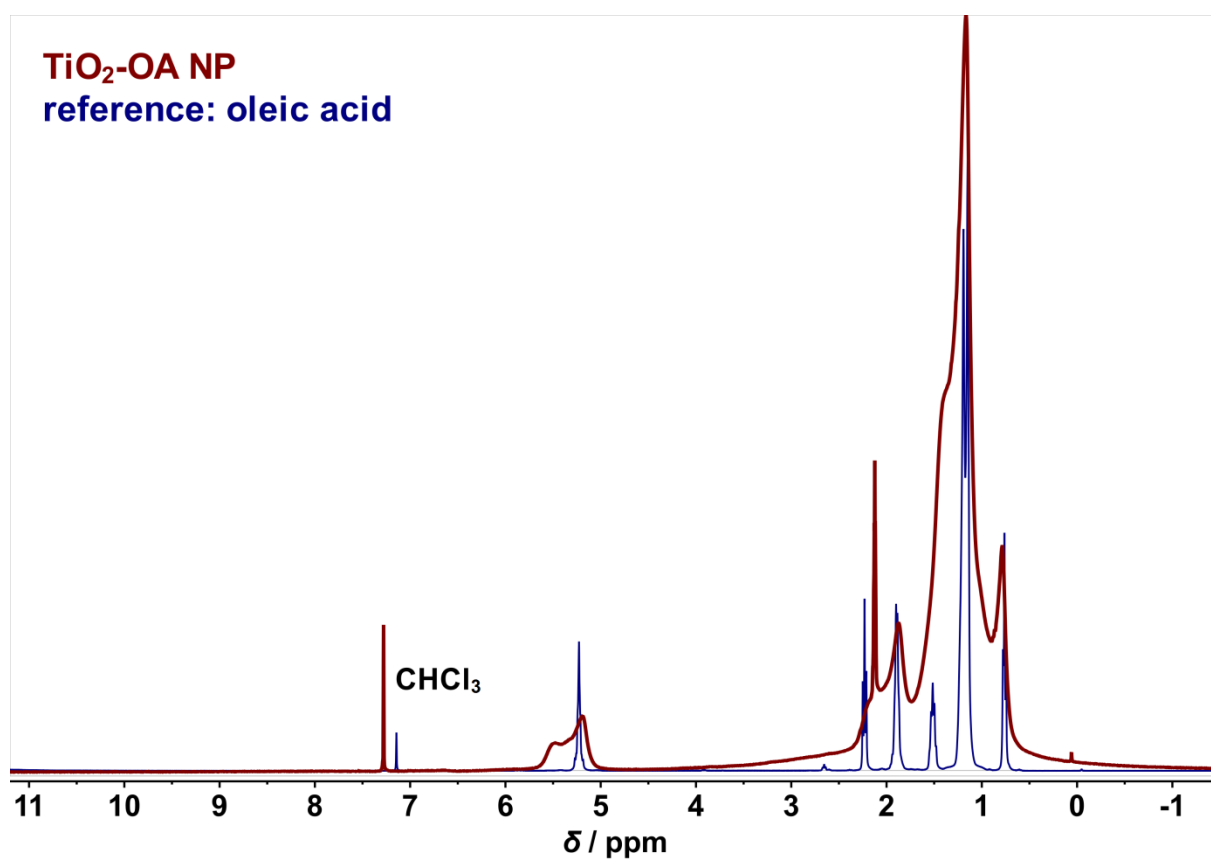


Figure S3. ¹H NMR spectra (400 MHz, CDCl₃) of TiO₂-OA NPs (maroon) and oleic acid reference (blue).

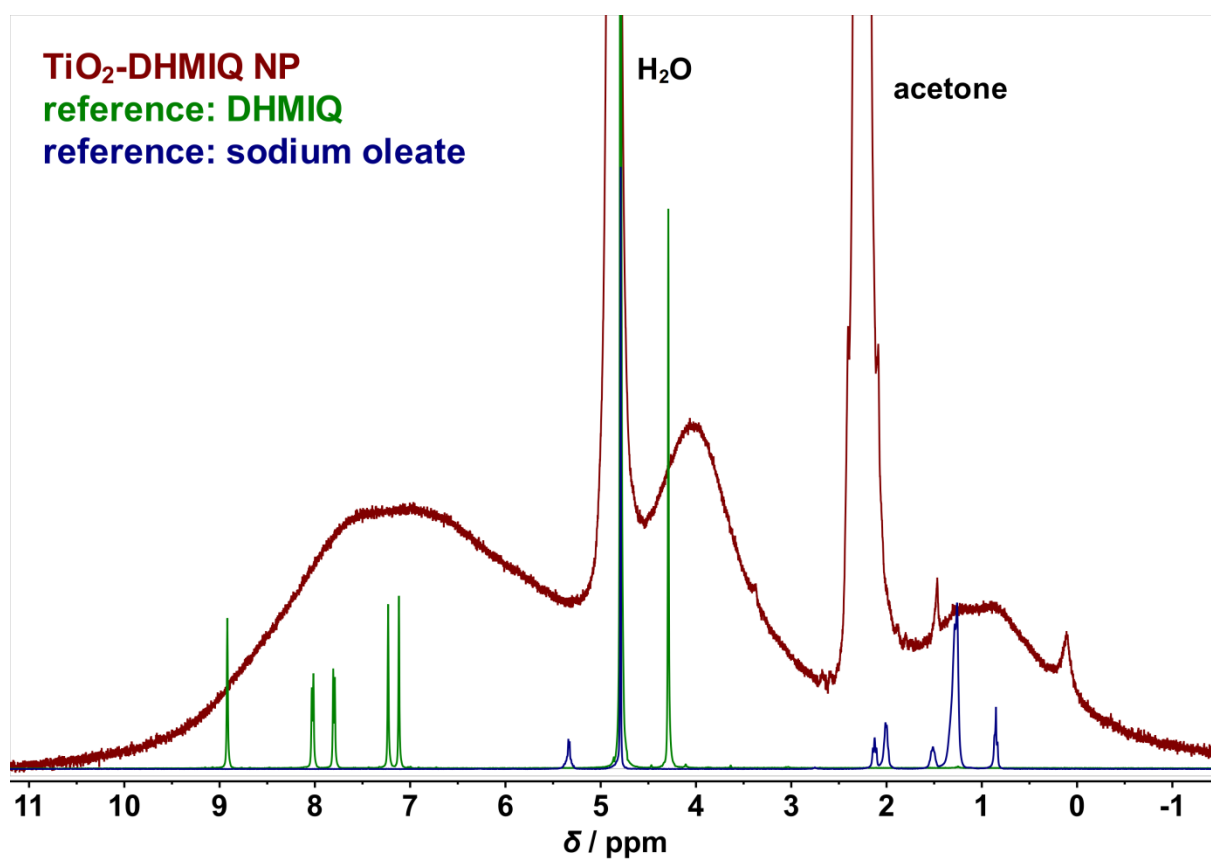


Figure S4. ¹H NMR spectra (400 MHz, D₂O) of TiO₂-DHMIQ NPs (maroon) and references of DHMIQ (green) and sodium oleate (blue).

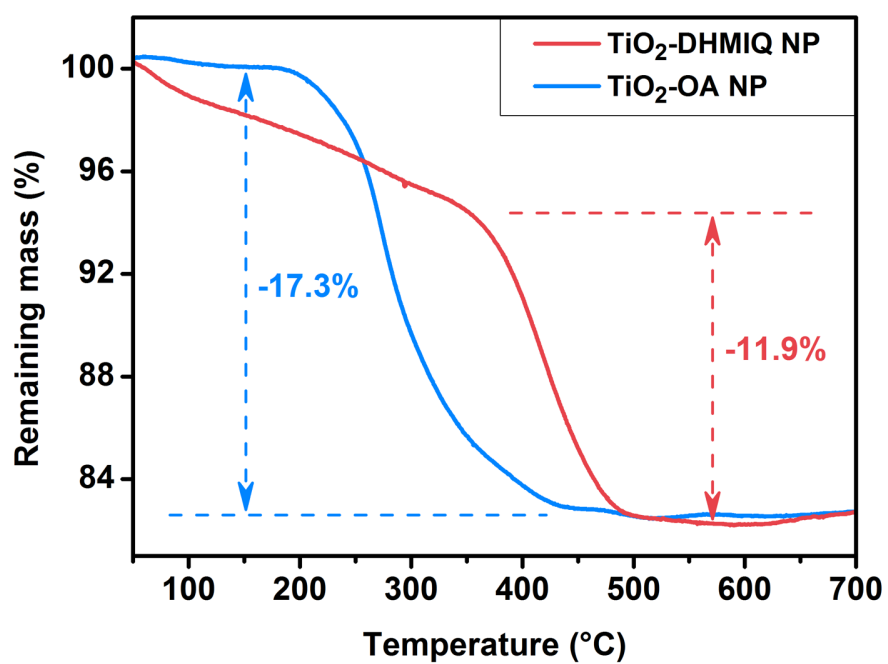


Figure S5. TGA profiles of TiO₂ nanoparticles before (blue curve, TiO₂-OA NP) and after DHMIQ modification (red curve, TiO₂-DHMIQ NP). The initial drop observed for the TiO₂-DHMIQ sample is presumably due to strongly adsorbed impurity species, such as H₂O.

Table S1. Characteristics of as-synthesized and DHMIQ-modified TiO₂ nanoparticles.

particle type	TiO ₂ -OA		TiO ₂ -DHMIQ	
major axis (nm) ^a	10.9	± 2.4	11.0	± 2.4
minor axis (nm) ^a	7.8	± 1.0	7.6	± 1.0
volume (nm ³) ^b	347	± 117	333	± 114
surface area (nm ²) ^b	243	± 56	238	± 56
specific surface area (m ² g ⁻¹)	153	± 63	166	± 69
organic fraction (%)	17.3	± 1.0	11.9	± 1.0
ligands per particle	588	± 202	486	± 171
ligand density (nm ⁻²)	2.4	± 1.0	2.0	± 0.9

^aMean values from TEM size evaluation after fitting individual particles as ellipses. ^bValues calculated according to the formulae for prolate (elongated) spheroids.

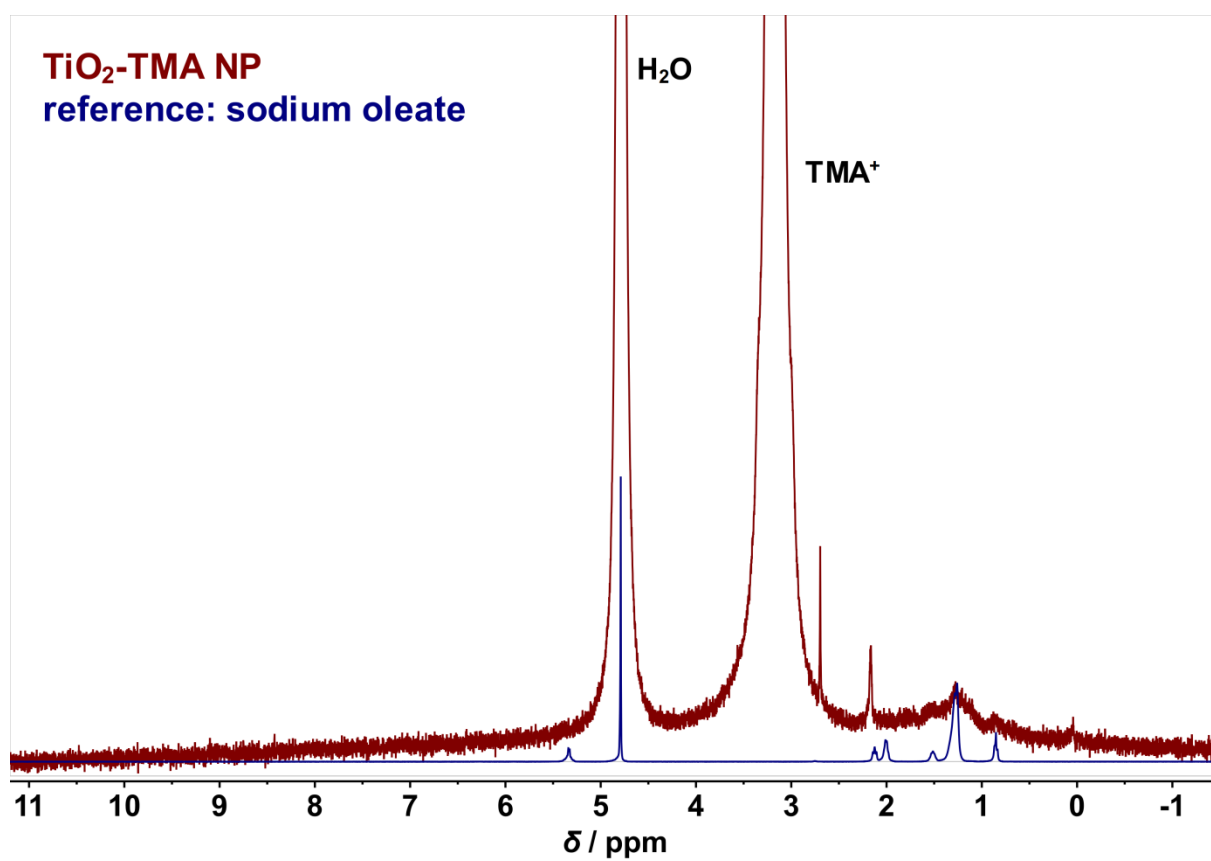


Figure S6. ¹H NMR spectra (400 MHz, D₂O) of TiO₂-TMA NPs (maroon) and sodium oleate reference (blue).

3. General Procedure & Setup

General procedure for the photocyanation of amines:

An aliquot of the TiO₂-DHMIQ solution (2.5 mg catalyst) was transferred in a reaction vial and freeze-dried. The dried catalyst was suspended with acetonitrile (4.0 mL) and the substrate (0.239 mmol, 1.0 eq.) was added. Oxygen was bubbled through the solution for one minute to saturate the solution. Trimethylsilyl cyanide (3.0 eq.) was added and the vial was closed tight. The solution was irradiated, if not stated otherwise, for 3 h, poured in concentrated NaHCO₃ solution (30 mL) and extracted with CH₂Cl₂ (3 x 20 mL). The combined organic layers were dried over Na₂SO₄ and the solvent was evaporated under reduced pressure to obtain the crude product. The pure product was isolated by filtration through a plug of aluminum oxide (basic) using CH₂Cl₂ as the eluent or by column chromatography.

Light sources:

- **HPR40E-48K100BG from Huey Jann Electronics Industry Co.:**
Blue LED, Power: 100 W, Voltage: max. 36 V, Light intensity: 2880 lm, $\lambda = 459\text{--}465\text{ nm}$ ($\lambda_{\text{max}} = 462\text{ nm}$).
- **HPR40E-43K100G from Huey Jann Electronics Industry Co.:**
Green LED, Power: 100 W, Voltage: max. 36 V, Light intensity: 6200 lm, $\lambda = 515\text{--}525\text{ nm}$ ($\lambda_{\text{max}} = 520\text{ nm}$).
- **Flood COB 50 Amber from Deko-Light Elektronik Vertriebs GmbH:**
Yellow LED, Power: 52 W, Voltage: max. 230 V, Light intensity: 1820 lm, Light efficiency: 34.85 lm/W, Angle of radiation 120°, $\lambda = 590\text{--}595\text{ nm}$ ($\lambda_{\text{max}} = 592\text{ nm}$).
- **RGB LED strips from LED-Konzept:**
Red LED, Power: 67 W, Voltage: max. 24 V, $\lambda_{\text{max}} = 635\text{ nm}$.
- **730 nm Infrared IR High Power LED Light:**
IR-LED, Power: 55 W, $\lambda = 720\text{--}740\text{ nm}$ ($\lambda_{\text{max}} = 730\text{ nm}$).
(<https://www.ebay.com/itm/690nm-730nm-760nm-790nm-810nm-850nm-940nm-100W-Infrared-IR-High-Power-LED-Light-/362216849137>).
Case: Himanjie 100 W LED Outdoor Flutlicht
(https://www.amazon.de/gp/product/B06Y4JMGXQ/ref=oh_aui_detailpage_o02_s00?ie=UTF8&psc=1).
- **IR-LED from Sygonix:**
IR-LED, Power: 3.6 W, Angle of radiation 45°, $\lambda_{\text{max}} = 850\text{ nm}$.

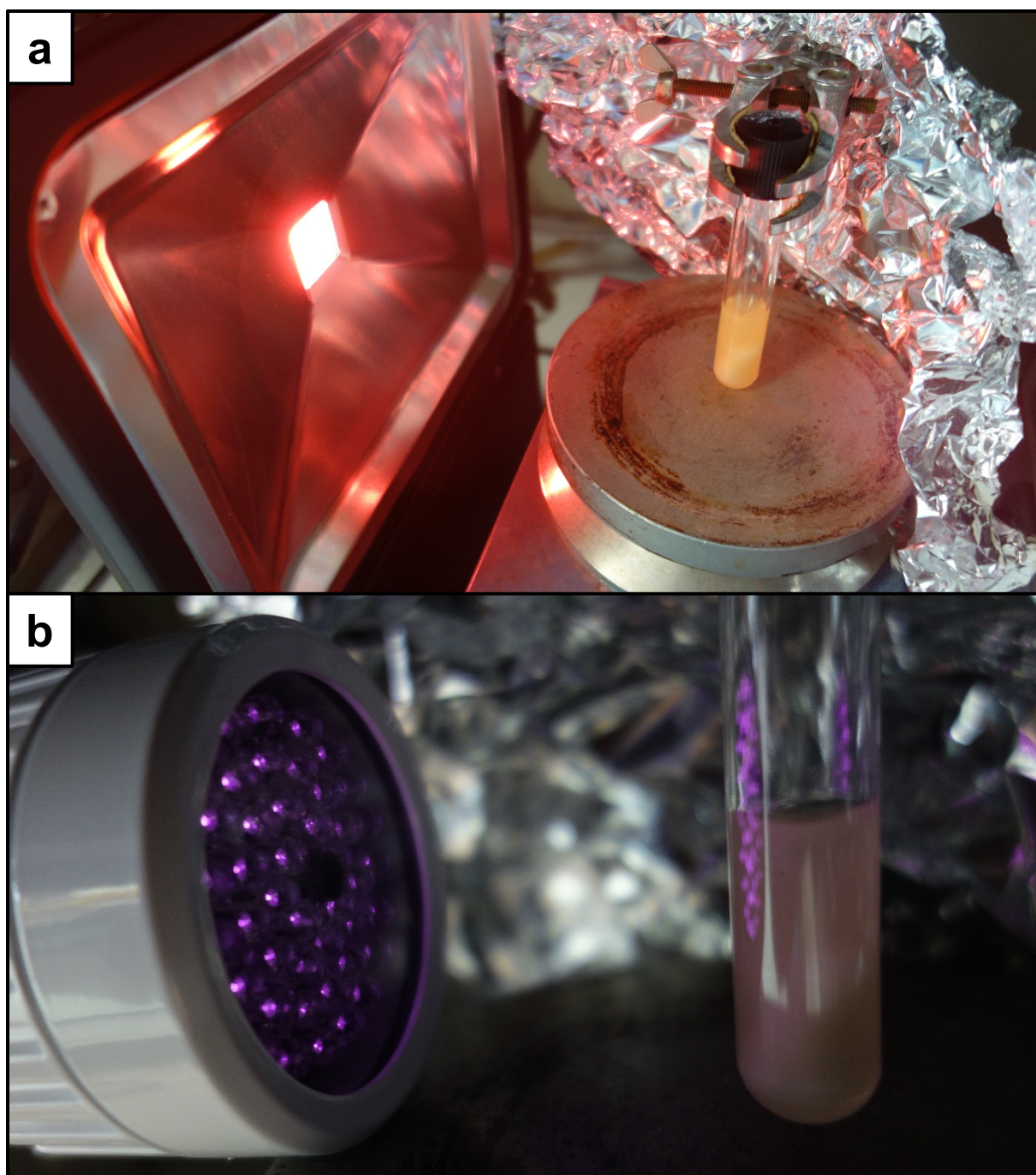
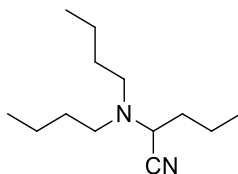


Figure S7. Photocyanation reactions with TiO_2 -DHMIQ under (a) NIR light (730 nm, ~15 cm distance between radiation source and reaction vessel) and (b) IR light (850 nm, ~7 cm distance between radiation source and reaction vessel).

4. Analytical Data

2-(Dibutylamino)-pentanenitrile (5):



The title compound was prepared according to the general procedure described above from *N*-butylamine (0.239 mmol, 1.0 equiv.). After purification by filtration through a plug of aluminum oxide (basic) using CH₂Cl₂ as the eluent, the product (48.2 mg, 0.229 mmol, 96%) was isolated as a colorless oil.

R_f = 0.70 (cyclohexane/ethyl acetate = 7:1).

IR (ATR): ν = 2959 (vs), 2932 (s), 2873 (m), 2221 (w), 1756 (w), 1467 (m), 1379 (w), 1173 (w), 1091 (w), 799 (w), 742 (w) cm⁻¹.

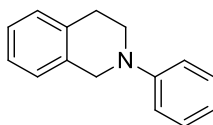
¹H NMR, COSY (300 MHz, CDCl₃): δ = 3.58 (t, ³*J*_{H-1a,H-2}=7.7 Hz, 1H, H-1a), 2.63–2.50 (m, 2H, H-1a'), 2.39–2.28 (m, 2H, H-1b'), 1.77–1.64 (m, 2H, H-2), 1.52–1.23 (m, 10H, H-3, H-2', H-3'), 0.99–0.82 (m, 9H, H-4, H-4') ppm.

¹³C NMR, HMBC, HSQC (75 MHz, CDCl₃): δ = 54.5 (C-1), 51.6 (C-1'), 34.1 (C-2), 30.4 (C-2'), 20.6 (C-3'), 19.5 (C-3), 14.1 (C-4'), 13.6 (C-4) ppm.

ESI-MS: *m/z* = 184.3 ([M–CN[−]], 18%), 211.2 ([M+H⁺], 100%).

The spectral data match those reported in the literature.⁶

2-Phenyl-1,2,3,4-tetrahydroisoquinoline (6):



To a stirred suspension of degassed 2-propanol (375 mL), ethylene glycol (42.0 mL, 46.6 g, 75.1 mmol, 4.0 equiv.), copper(I)iodide (3.58 g, 18.8 mmol, 0.1 equiv.) and tribasic potassium phosphate (79.7 g, 375 mmol, 2.0 equiv.), 1,2,3,4-tetrahydroisoquinoline (25.0 g, 188 mmol, 1.0 equiv.) and iodobenzene (38.3 g, 188 mmol, 1.0 equiv.) were added. The mixture was heated to 90 °C for 24 h. After cooling, the suspension to room temperature the solvent was removed by rotary evaporation. The residue was diluted with water (280 mL) and extracted five times with dichloromethane (50 mL). The combined organic layers were washed with brine, dried over sodium sulfate and evaporated into dryness. The crude product was purified by column chromatography on silica gel (cyclohexane/ethyl acetate = 50:1) to yield the product (28.9 g, 138 mmol, 73%) as a slightly yellow solid.

mp.: 41.4–42.9 °C. Lit.: 44–46 °C.⁷

R_f = 0.19 (cyclohexane/ethyl acetate = 50:1).

IR (ATR): ν = 3062 (m), 3024 (m), 2901 (m), 2817 (m), 1598 (vs), 1502 (vs), 1463 (m), 1388 (m), 1225 (m), 931 (w), 752 (vs), 692 (s) cm^{-1} .

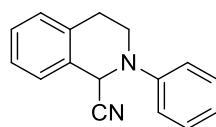
¹H NMR, COSY (300 MHz, CDCl_3): δ = 7.51–7.44 (m, 2H, H-3', 5'), 7.38–7.28 (m, 4H, H-5, H-6, H-7, H-8), 7.18–7.13 (m, 2H, H-2', 6'), 7.03 (tt, $^3J_{\text{Ph-4, Ph-3/5}}$ = 7.2 Hz, $^4J_{\text{Ph-4, Ph-2/6}}$ = 1.1 Hz, 1H, H-4'), 4.56 (s, 2H, H-1), 3.70 (t, $^3J_{\text{H-3, H-4}}$ = 5.9 Hz, 2H, H-3), 3.13 (t, $^3J_{\text{H-4, H-3}}$ = 5.9 Hz, 2H, H-4) ppm.

¹³C NMR, HMBC, HSQC (75 MHz, CDCl_3): δ = 150.4 (C-1'), 134.8, 134.4 (C-4a, C-8a), 129.2 (C-3', 5'), 128.5, 126.5, 126.3, 126.0 (C-5, C-6, C-7, C8), 118.7 (C-4'), 115.1 (C-2', 6'), 50.7 (C-1), 46.5 (C-3), 29.1 (C-4) ppm.

ESI-MS: m/z = 210.1 ($[\text{M}+\text{H}^+]$, 100%), 208.1 ($[\text{M}-\text{H}^-]$, 39%).

The spectral data match those reported in the literature.⁷

2-Phenyl-1,2,3,4-tetrahydroisoquinoline-1-carbonitrile (14):



The title compound was prepared according to the general procedure described above from 2-phenyl-1,2,3,4-tetrahydroisoquinoline (44 mg, 0.21 mmol, 1.0 equiv.). After column chromatography (cyclohexane/ethyl acetate = 20:1) the product (42.8 mg, 0.183 mmol, 87%) was isolated as a colorless solid.

mp: 98.1–99.5 °C. Lit.: 95–96 °C.⁸

R_f = 0.27 (cyclohexane/ethyl acetate = 20:1).

IR (ATR): ν = 3064 (w), 3028 (w), 2828 (w), 2834 (w), 1598 (s), 1502 (s), 1427 (m), 1222 (m), 1202 (m), 938 (m), 741 (s), 693 (m) cm^{-1} .

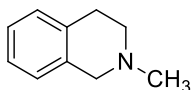
¹H NMR, COSY (300 MHz, CDCl_3): δ = 7.41–7.22 (m, 6H, Ar-H, H-3', 5'), 7.13–7.07 (m, 2H, H-2', 6'), 7.06–6.99 (m, 1H, H-4'), 5.53j (s, 1H, H-1), 3.79 (dddd, $^2J_{\text{H-3a, H-3b}}$ = 12.4 Hz, $^3J_{\text{H-3a, H-4}}$ = 5.9, 3.0 Hz, $^4J_{\text{H-3a, H-1}}$ = 1.1 Hz, 1H, H-3_a), 3.50 (ddd, $^2J_{\text{H-3b, H-3a}}$ = 12.4 Hz, $^3J_{\text{H-3b, H-4}}$ = 10.6, 4.1 Hz, 1H, H-3_b), 3.18 (ddd, $^2J_{\text{H-4a, H-4b}}$ = 16.4 Hz, $^3J_{\text{H-4a, H-3}}$ = 10.6, 5.9 Hz, 1H, H-4_a), 2.98 (dt, $^2J_{\text{H-4b, H-4a}}$ = 16.4 Hz, $^3J_{\text{H-4b, H-3}}$ = 3.6 Hz, 1H, H-4_b) ppm.

¹³C NMR, HMBC, HSQC (75 MHz, CDCl_3): δ = 148.5 (C-1'), 134.8 (C-4a, C-8a), 129.7 (C-3', 5'), 129.5 (C-5), 128.9, 127.2, 127.0 (C-6, C-7, C8), 122.0 (C-4'), 117.9 (CN), 117.7 (C-2', 6'), 53.4 (C-1), 44.3 (C-3), 28.7 (C-4) ppm.

ESI-MS: m/z = 208.1 ($[\text{M}-\text{CN}^-]$, 100%), 235.2 ($[\text{M}+\text{H}^+]$, 52%).

The spectral data match those reported in the literature.⁹

2-Methyl-1,2,3,4-tetrahydroisoquinoline (7):



At 0 °C, formic acid (17.28 g, 375 mmol, 14.16 mL, 2.00 eq.), formaldehyde solution (16.77 mL, 207 mmol, 1.1 eq.) and 1,2,3,4-tetrahydroisoquinoline (25.00 g, 188 mmol, 23.81 mL, 1.0 eq) were combined and heated to 80 °C for 24 h. After cooling to 0 °C, the solution was poured in half concentrated hydrochloric acid (100 mL) and extracted with diethyl ether (3 x 100 mL). The aqueous solution was basified with sodium hydroxide solution (2 M) and extracted with diethyl ether (3 x 100 mL). The combined organic layers were dried over sodium sulfate and concentrated in vacuo to yield the crude product. The purification was performed by Kugelrohr distillation (121 °C, 23 mbar) under vacuum to yield the title product (19.17 g, 130.3 mmol, 69%).

Bp: 121 °C (23 mbar).

R_f = 0.65 (cyclohexane/ethyl acetate/triethylamine = 2:4:1).

IR (ATR): ν = 2919 (m), 2779 (m), 1498 (m), 1427 (m), 1347 (m), 1290 (m), 1099 (m), 936 (m), 738 (vs) cm^{-1} .

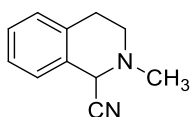
¹H NMR, COSY (300 MHz, CDCl₃): δ = 7.14–7.09 (m, 3H, Ar-H), 7.03–7.01 (m, 1H, Ar-H), 3.60 (s, 2H, H-1), 2.94 (t, $^3J_{\text{H-3, H-4}}$ = 5.9 Hz, 2H, H-3), 2.70 (t, $^3J_{\text{H-3, H-4}}$ = 5.9 Hz, 2H, H-4), 2.47 (s, 3H, N-CH₃) ppm.

¹³C NMR, HMBC, HSQC (75 MHz, CDCl₃): δ = 134.7 (C-4a), 133.8 (C-8a), 128.7 (C-5), 126.5 (C-6), 126.2 (C-8), 125.7 (C-7), 58.0 (C-1), 52.99 (C-3), 46.2 (N-CH₃), 26.2 (C-4) ppm.

ESI-MS: m/z = 148.2 ([M-H⁺], 100%).

The spectral data match those reported in the literature.¹⁰

2-Methyl-1,2,3,4-tetrahydroisoquinoline-1-carbonitrile (15):



The title compound was prepared according to the general procedure described above from 2-methyl-1,2,3,4-tetrahydroisoquinoline (0.239 mmol, 1.0 equiv.). After purification by filtration through a plug of aluminum oxide (basic) using CH₂Cl₂ as the eluent, the product (33.4 mg, 0.227 mmol, 95%) was isolated as a colorless oil.

R_f = 0.56 (cyclohexane/ethyl acetate/triethylamine = 1:3:0.1).

IR (ATR): ν = 2981 (s), 2857 (s), 2809 (s), 2225 (w), 1498 (m), 1455 (m), 1148 (m), 1102 (m), 1067 (w), 945 (w), 853 (m) cm^{-1} .

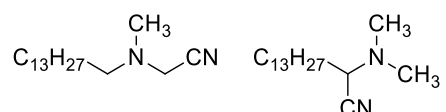
¹H NMR, COSY (300 MHz, CDCl₃): δ = 7.29–7.13 (m, 4H, H-5, H-6, H-7, H-8), 4.73 (s, 1H, H-1), 3.12–2.97 (m, 1H, H-4_a), 2.94–2.75 (m, 3H, H-3, H-4_b), 2.60 (s, 3H, CH₃) ppm.

¹³C NMR, HMBC, HSQC (75 MHz, CDCl₃): δ = 133.9 (C-4a), 129.6 (C-8a), 129.4, 128.5, 126.5 (C-5, C-6, C-7), 127.1 (C-8), 116.5 (CN), 56.9 (C-1), 48.4 (C-3), 43.7 (CH₃), 27.4 (C-4) ppm.

ESI-MS: m/z = 173.1 ([M+H⁺], 100%), 146.1 ([M–CN⁺], 78%).

The spectral data match those reported in the literature.¹¹

[Tetradecyl(methyl)amino]acetonitrile and 2-(dimethylamino)pentadecanenitrile (16, 17):



The title compound was prepared according to the general procedure described above from *N,N*-dimethyl-tetradecylamine (0.239 mmol, 1.0 equiv.). After purification by filtration through a plug of aluminum oxide (basic) using CH₂Cl₂ as the eluent, the product (48.2 mg, 0.229 mmol, 96%) was isolated as a colorless oil as a mixture of [tetradecyl(methyl)amino]acetonitrile and 2-(dimethylamino)pentadecanenitrile with a ratio of 29:71.

R_f = 0.81 (CH₂Cl₂/MeOH, 10:1).

IR (ATR): ν = 2923 (s), 2850 (s), 2812 (m), 2213 (w), 1475 (m), 1369 (w), 1326 (m), 1039 (m) cm⁻¹.

ESI-MS: m/z = 267.2 ([M+H⁺], 100%), 240.3 ([M–CN⁺], 43%).

[Tetradecyl(methyl)amino]acetonitrile:

¹H NMR, COSY (300 MHz, CDCl₃): δ = 3.53 (s, 2H, H-1), 2.43 (t, ³J_{H-1', H-2'} = 7.2 Hz, 1H, H-2), 2.34 (s, 3H, H-1''), 1.50–1.36 (m, 2H, H-2'), 1.35–1.19 (m, 22H, H-3', H-4', H-5', H-6', H-7', H-8', H-9', H-10', H-11', H-12', H-13'), 0.87 (s, 3H, H-14') ppm.

¹³C NMR, HMBC, HSQC (75 MHz, CDCl₃): δ = 114.8 (CN), 56.0 (C-1'), 45.3 (C-1), 42.2 (C-1''), 27.6 (C-2'), 31.1, 29.9–29.4, 27.2, 22.8 (C-3', C-4', C-5', C-6', C-7', C-8', C-9', C-10', C-11', C-12', C-13'), 14.3 (C-14') ppm.

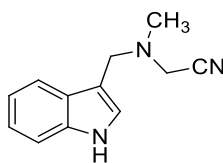
2-(Dimethylamino)pentadecanenitrile:

¹H NMR, COSY (300 MHz, CDCl₃): δ = 3.46 (t, ³J_{H-2, H-3} = 7.4 Hz, 1H, H-2), 2.30 (s, 6H, H-1', H-1''), 1.78–1.66 (m, 2H, H-3), 1.50–1.36 (m, 2H, H-4), 1.35–1.19 (m, 20H, H-5, H-6, H-7, H-8, H-9, H-10, H-11, H-12, H-13, H-14), 0.87 (s, 3H, H-15) ppm.

¹³C NMR, HMBC, HSQC (75 MHz, CDCl₃): δ = 117.0 (C-1), 58.9 (C-2), 41.9 (C-1', C-1''), 31.8 (C-3), 26.1 (C-4), 29.9–29.4, 29.1 (C-5, C-6, C-7, C-8, C-9, C-10, C-11, C-12, C-13, C-14), 14.3 (C-15) ppm.

The spectral data match those reported in the literature.^{6,12}

[(1*H*-indol-3-ylmethyl)(methyl)amino]acetonitrile (18):



The title compound was prepared according to the general procedure described above from Gramine (0.239 mmol, 1.0 equiv.). After column chromatography by flash chromatography on silica gel (CH₂Cl₂/MeOH, 20:1) the product was isolated as a colorless oil (42.4 mg, 0.213 mmol, 89%).

R_f = 0.65 (CH₂Cl₂/MeOH = 10:1).

IR (ATR): ν = 3405 (s), 2951 (s), 2788 (m), 2222 (w), 1670 (m), 1450 (m), 1342 (m), 844 (m), 741 (w) cm⁻¹.

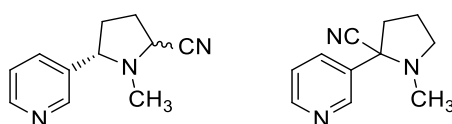
¹H NMR, COSY (300 MHz, CDCl₃): δ = 8.12 (s_{br}, 1H, NH), 7.74 (d, ³*J*_{H-4, H-5} = 7.7 Hz, 1H, H-4), 7.39 (d, ³*J*_{H-7, H-6} = 7.4 Hz, 1H, H-7), 7.25–7.19 (m, 2H, H-2, H-6), 7.14 (m, 1H, H-5) 3.81 (s, 2H, H-8), 3.46 (s, 2H, H-9), 2.50 (s, 3H, N-10) ppm.

¹³C NMR, HMBC, HSQC (75 MHz, CDCl₃): δ = 136.5 (C-7a), 127.2 (C-3a), 124.0 (C-2), 122.5 (C-6), 119.9 (C-5), 119.5 (C-4), 114.8 (CN), 111.9 (C-3), 111.2 (C-7), 51.2 (C-8), 43.7 (C-9), 42.4 (C-10) ppm.

ESI-MS: *m/z* = 173.0 ([M–CN]⁺, 100%).

The spectral data match those reported in the literature.¹²

1-Methyl-5-(pyridin-3-yl)pyrrolidine-2-carbonitrile and 1-methyl-2-(pyridin-3-yl)pyrrolidine-2-carbonitrile (19, 20):



The title compound was prepared according to the general procedure described above from nicotine (0.239 mmol, 1.0 equiv.). After purification by filtration through a plug of aluminum oxide (basic) using CH₂Cl₂ as the eluent, the product (38.1 mg, 0.203 mmol, 85%) was isolated as a colorless oil as a mixture of 1-methyl-2-(pyridin-3-yl)pyrrolidine-2-carbonitrile and both diastereomeres 1-methyl-5-(pyridin-3-yl)pyrrolidine-2-carbonitrile with a ratio of 56:28:16.

R_f = 0.39 (ethyl acetate).

ESI-MS: *m/z* = 188.0 ([M+H]⁺, 100%), 161.1 ([M–CN]⁺, 49%).

1-Methyl-2-(pyridin-3-yl)pyrrolidine-2-carbonitrile:

¹H NMR, COSY (300 MHz, CDCl₃): δ = 8.84 (dd, ⁴*J*_{H-2', H-4'} = 2.5 Hz, ⁴*J*_{H-2', H-6'} = 0.9 Hz, 1H, H-2'), 8.60 (dd, ³*J*_{H-6', H-5'} = 4.8 Hz, ⁴*J*_{H-6', H-4'} = 1.6 Hz, 1H, H-6'), 7.88 (ddd, ³*J*_{H-4', H-5'} = 8.0 Hz,

$^4J_{\text{H-4}', \text{H-2}'} = 2.5 \text{ Hz}$, $^4J_{\text{H-4}', \text{H-6}'} = 1.6 \text{ Hz}$, 1H, H-4'), 7.35–7.24 (m, 1H, H-5'), 3.41–3.28 (m, 1H, H-5_a), 2.76–2.62 (m, 1H, H-5_b), 2.61–2.52 (m, 1H, H-3_a), 2.23 (s, 3H, CH₃), 2.14–1.99 (m, 3H, H-3_b, H-4) ppm.

¹³C NMR, HMBC, HSQC (75 MHz, CDCl₃): $\delta = 150.1$ (C-6'), 148.1 (C-2'), 134.1 (C-4'), 133.9 (C-2'), 123.6 (C-5'), 117.0 (CN), 69.8 (C-2), 53.9 (C-5), 43.2 (C-3), 36.3 (CH₃), 21.2 (C-4) ppm.

1-Methyl-5-(pyridin-3-yl)pyrrolidine-2-carbonitrile – major diastereomer:

¹H NMR, COSY (300 MHz, CDCl₃): $\delta = 8.56$ –8.50 (m, 2H, H-2', H-6'), 7.64 (dt, $^3J_{\text{H-4}', \text{H-5}'} = 7.8 \text{ Hz}$, $^4J_{\text{H-4}', \text{H-2}'/\text{H-6}'} = 2.0 \text{ Hz}$, 1H, H-4'), 7.35–7.24 (m, 1H, H-5'), 4.18–4.10 (m, 1H, H-2), 3.57 (t, $^3J_{\text{H-5}, \text{H-4}} = 8.0 \text{ Hz}$, 1H, H-5), 2.48–2.43 (m, 1H, H-4_a), 2.41–2.27 (m, 1H, H-3_a), 2.31 (s, 3H, CH₃), 2.23–2.13 (m, 1H, H-3_b), 1.83–1.75 (m, 1H, H-4_b) ppm.

¹³C NMR, HMBC, HSQC (75 MHz, CDCl₃): $\delta = 149.4$ (C-6'), 149.3 (C-2'), 137.5 (C-3'), 134.9 (C-4'), 123.9 (C-5'), 117.5 (CN), 65.2 (C-5), 56.8 (C-2), 39.0 (CH₃), 33.3 (C-4), 28.5 (C-3) ppm.

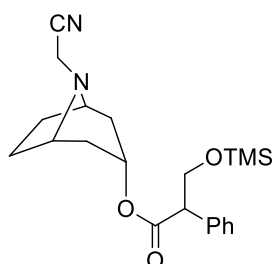
1-Methyl-5-(pyridin-3-yl)pyrrolidine-2-carbonitrile – minor diastereomer:

¹H NMR, COSY (300 MHz, CDCl₃): $\delta = 8.56$ –8.50 (m, 2H, H-2', H-6'), 7.73 (dt, $^3J_{\text{H-4}', \text{H-5}'} = 7.91 \text{ Hz}$, $^4J_{\text{H-4}', \text{H-2}'/\text{H-6}'} = 2.0 \text{ Hz}$, 1H, H-4'), 7.35–7.24 (m, 1H, H-5'), 3.41–3.28 (m, 3H, H-2, H-5), 2.41–2.27 (m, 1H, H-3_a), 2.30–2.23 (m, 1H, H-4_a), 2.29 (s, 3H, CH₃), 2.23–2.13 (m, 1H, H-3_b), 1.92–1.80 (m, 1H, H-4_b) ppm.

¹³C NMR, HMBC, HSQC (75 MHz, CDCl₃): $\delta = 149.5$ (C-6'), 149.4 (C-2'), 137.0 (C-3'), 134.7 (C-4'), 123.8 (C-5'), 120.2 (CN), 68.2 (C-5), 55.9 (C-2), 36.6 (CH₃), 34.3 (C-4), 28.7 (C-3) ppm.

The spectral data match those reported in the literature.¹²

8-(Cyanomethyl)-8-azabicyclo[3.2.1]oct-3-yl 2-phenyl-3-[(trimethylsilyl)oxy]propanoate (21):



Atropine base was isolated from Atropine sulfate monohydrate as described in literature. The atropine base (60.8 mg, 0.21 mmol, 1.0 equiv.) was cyanated according to the general procedure described above. The crude product was purification by column chromatography on silica gel (chloroform/methanol = 20:1) and the product (51.0 mg, 0.132 mmol, 63%) was isolated as a slightly yellow oil. The product decomposes on the column by deprotection.

$R_f = 0.62$ (chloroform/methanol = 20:1).

IR (ATR): $\nu = 2950$ (w), 2878 (w), 2245 (w), 1727 (s), 1667 (w), 1251 (s), 1201 (s), 1170 (s), 1155 (s), 1102 (s), 1080 (m), 1065 (s), 1034 (s), 894 (m), 839 (s), 779 (m), 699 (s) cm^{-1} .

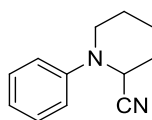
¹H NMR, COSY (400 MHz, CDCl₃): δ = 7.33–7.23 (m, 5H, Ar-H), 4.98 (t, ³J_{H-3, H-2a & H-4a} = 5.5 Hz, 1H, H-3), 4.20–4.12 (m, 1H, H-3a'), 3.78–3.70 (m, 2H, H-2', H-3b'), 3.27–3.13 (m, 2H, H-1, H-5), 3.23 (s, 2H, N-CH₂-CN), 2.15–1.56 (m, 8H, H-2, H-4, H-6, H-7), 0.07 (s, 9-H, TMS) ppm.

¹³C NMR, HMBC, HSQC (100 MHz, CDCl₃): δ = 171.5 (CO), 135.6 (Ph-1), 128.6, 127.9 (Ph-2, Ph-3, Ph-5, Ph-6), 127.5 (Ph-4), 117.3 (CN), 67.3 (C-3), 64.5 (C-3'), 58.7, 58.6 (C-1, C-5), 54.7 (C-2'), 40.8 (N-CH₂-CN), 36.7, 36.4 (C-2, C-4), 25.2, 24.9 (C-6, C-7), –0.75 (SiCH₃) ppm.

ESI-MS: m/z = 387.2 ([M+H⁺], 100%).

The spectral data match those reported in the literature.¹²

1-Phenylpiperidine-2-carbonitrile (22):



The title compound was prepared according to the general procedure described above from 1-Phenylpiperidine (0.239 mmol, 1.0 equiv.). After column chromatography on silica gel (cyclohexane/ethyl acetate = 5:1) the product was isolated as a brown oil (37.8 mg, 0.203 mmol, 85%).

R_f = 0.35 (cyclohexane/ethyl acetate = 7:1).

¹H NMR, COSY (300 MHz, CDCl₃): δ = 7.33–7.25 (m, 2H, H-3', H-5'), 7.01–6.89 (m, 3H, H-2', H-4', H-6'), 4.62 (t, ³J_{H-2, H-3} = 3.5 Hz, 1H, H-2), 3.48–3.38 (m, 1H, H-6_a), 3.03–2.93 (m, 1H, H-6_b), 2.03–1.89 (m, 2H, H-3), 1.87–1.60 (m, 4H, H-4, H-5) ppm.

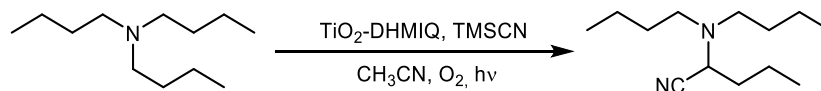
¹³C NMR, HMBC, HSQC (75 MHz, CDCl₃): δ = 149.5 (C-1'), 129.1 (C-3', C-5), 122.0 (C-4'), 118.3 (C-2', 5'), 117.2 (CN), 51.7 (C-2), 46.2 (C-6), 29.3 (C-3), 24.9 (C-4), 20.0 (C-5) ppm.

ESI-MS: m/z = 160.1 ([M–CN[–]], 100%).

The spectral data match those reported in the literature.¹³

5. Reaction Screening

Reaction screening with the cyanation of tributylamine:



5.1. Catalyst loading

Table S2. Influence of the catalyst loading on the reaction yield.

Catalyst	2.5 mg	1.0 mg	0.5 mg	0.2 mg	0.1 mg	0.05 mg	0.02 mg	0.01 mg	0.0 mg
Yield	95%	59%	51%	47%	41%	30%	27%	25%	14%

Reaction conditions: Bu₃N (0.239 mmol, 1.0 eq.) and dry TiO₂-DHMIQ were mixed in acetonitrile (4.0 mL). The suspension was saturated with oxygen and TMSCN (3.0 eq.) was added. The reaction vial was closed and irradiated with blue light for 3 h. The crude product was isolated by extraction and the yield was determined by ¹H NMR spectroscopy with 1,4-bis(trimethylsilyl)benzene as internal standard.

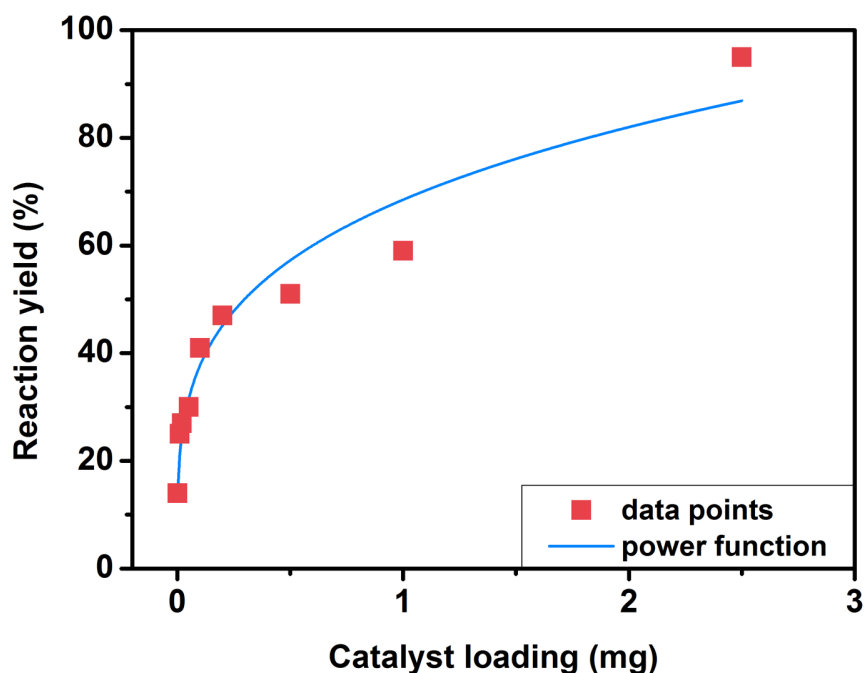


Figure S8. Effect of catalyst loading on reaction yield.

The effect of catalyst loading on reaction yield was fitted with a power-type function:

$$\frac{r}{\%} = a \left(\frac{m}{\text{mg}} \right)^b$$

where

- r = reaction yield (in %),
- m = catalyst mass (in mg),
- $a = 68.51$,
- $b = 0.26$.

This type of function is a widely used expression in the field of catalysis to describe adsorption processes on solid surfaces (cf. Freundlich adsorption isotherm).¹⁴ It should be noted, however, that this is only a simplistic mathematical approximation of a complex correlation, which has not been studied in detail.

5.2. Influence of water

Table S3. Influence of water on the catalysis efficiency of TiO₂-DHMIQ.

Water addition	0 μL	1 μL	5 μL	10 μL	20 μL	40 μL
Yield	95%	61%	27%	19%	19%	20%

Reaction conditions: Bu₃N (0.239 mmol, 1.0 eq.), dry TiO₂-DHMIQ (2.5 mg) and water were mixed in acetonitrile (4.0 mL). The suspension was saturated with oxygen and TMSCN (3.0 eq.) was added. The reaction vial was closed and irradiated with blue light for 3 h. The crude product was isolated by extraction and the yield was determined by ¹H NMR spectroscopy with 1,4-bis(trimethylsilyl)benzene as internal standard.

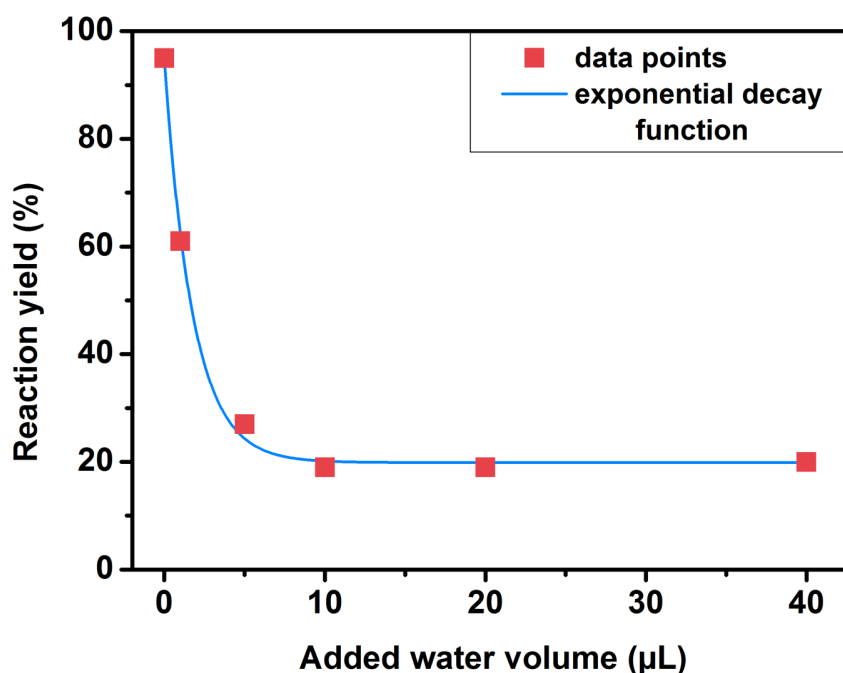


Figure S9. Effect of water addition on reaction yield.

The effect of water on reaction yield was fitted with an exponential decay function:

$$\frac{r}{\%} = a \cdot \exp\left(-b \frac{V}{\mu\text{L}}\right) + c$$

where

- r = reaction yield (in %),
- V = water volume (in μL),
- $a = 74.52$,
- $b = 0.56$,
- $c = 19.89$.

The use of an exponential decay function is justified by the observation that the conversion dropped much faster for small amounts of water than for higher amounts. The most plausible explanation for this behavior is the formation of a hydration shell around the polar nanoparticles, thus passivating the surface and preventing the substrate molecules from approaching the reactive sites. Since the hydration shell has a finite maximum thickness, the conversion is not completely suppressed for higher amounts of water, but levels off to a conversion rate of approximately 20%.

This assumption is supported by the fact that 1 μL of added water corresponds to a hydration shell thickness of 2–3 nm (*vide infra* for details on the calculation).^{*} This value is in accordance with experimental results, where hydration layer thicknesses of up to 4 nm were observed on alumina nanoparticles.¹⁵ Given the fact that the uncharged substrate molecules (such as tributylamine) have only a moderate polarity, a hydration layer of several nm thickness constitutes a considerable energy barrier for the molecules to approach the nanoparticle surface. This is why such a small amount as 1 μL of water is sufficient to reduce the reaction yield by 34%. Eventually, the reaction yield levels off at approximately 20% beyond 5 μL of water added. This volume corresponds to a hydration layer of ~ 12 nm, which is a plausible maximum value for a highly charged surface in the otherwise apolar environment of acetonitrile. Consequently, further addition of water has little effect on reaction yield as it does not add to the hydration shell anymore, but instead mixes with acetonitrile.

Although hydrolysis of TMSCN will certainly occur, it is not likely the main reason for the observed decrease of the reaction yield. Addition of 1 μL of water (0.06 mmol) would only cause 8 mol% of the employed TMSCN (0.72 mmol) to hydrolyze while at the same time the reaction yield drops by 34%.

^{*}The hydration shell thickness was calculated as follows:

$$d = \frac{V}{A} = \frac{V}{A_s \cdot m} = \frac{10^{-9} \text{ m}^3}{166 \text{ m}^2\text{g}^{-1} \cdot 2.5 \cdot 10^{-3} \text{ g}} = 2.4 \cdot 10^{-9} \text{ m} = 2.4 \text{ nm}$$

where

d = hydration shell thickness,

V = water volume (1 μL = 10^{-9} m^3),

A = surface area,

A_s = specific surface area (see Table S1: $166 \text{ m}^2\text{g}^{-1}$),

m = catalyst mass (2.5 mg).

5.3. Catalyst recovery

Table S4. Recovery and reuse of the catalyst.

Cycle	1	2	3	4
Yield	95%	92%	87%	82%

Reaction conditions: Bu₃N (0.239 mmol, 1.0 eq.) and dry TiO₂-DHMIQ (2.5 mg) were mixed in acetonitrile (4.0 mL). The suspension was saturated with oxygen and TMSCN (3.0 eq.) was added. The reaction vial was closed and irradiated with blue light for 3 h. The catalyst was precipitated, isolated by centrifugation (4700 rpm, 10 min, −9 °C) and suspended in acetonitrile (4.0 mL). This washing procedure was repeated twice, before the catalyst was reused. The crude product was isolated by extraction from all combined acetonitrile phases and the yield was determined by ¹H NMR spectroscopy with 1,4-bis(trimethylsilyl)benzene as internal standard.

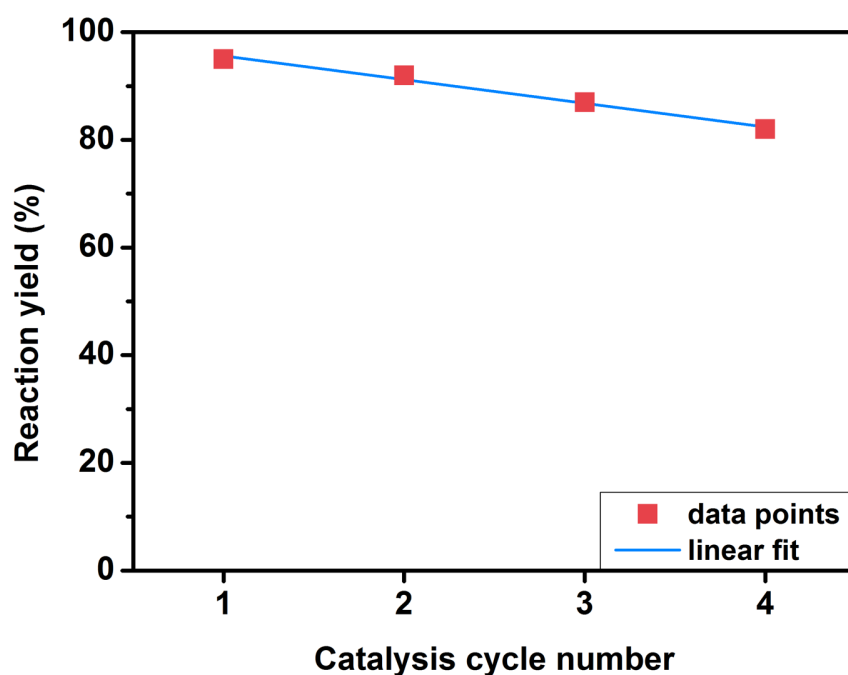


Figure S10. Effect of catalyst recycling on reaction yield.

The effect of catalyst recycling on reaction yield was fitted with a linear function:

$$\frac{r}{\%} = a \cdot x + b$$

where

r = reaction yield (in %),

x = cycle number,

$a = -4.4$,

$b = 100$.

The decrease in catalytic performance follows a linear decay function, presumably due to gradual degradation of the photocatalyst, such as self-oxidation.

5.4. Additional screenings

Table S5. Additional screening conditions.

Entry	Notification	Yield
1	No light ^[a]	>1%
2	No light ^[a] , 16 h	6%
3	No light, 50 °C	2%
4	No light, 100 °C	9%
5	No light & no catalyst, 50 °C	2%
6	No light & no catalyst, 100 °C	12%
7	2.00 mg Ligand ^[b]	53%
8	0.29 mg DHMIQ (= 0.57 mol%)	84%
9	0.06 mg DHMIQ (= 0.12 mol%)	80%
10	0.29 mg DHMIQ (= 0.57 mol%) + TiO ₂ -TMA (2.2 mg)	62%

Reaction conditions: Bu₃N (0.239 mmol, 1.0 eq.) and dry TiO₂-DHMIQ were mixed in acetonitrile (4.0 mL). The suspension was saturated with oxygen and TMSCN (3.0 eq.) was added. The reaction vial was closed and irradiated with blue light for 3 h. The crude product was isolated by extraction and the yield was determined by ¹H NMR spectroscopy with 1,4-bis(trimethylsilyl)benzene as internal standard. ^[a]The reaction vial was wrapped in aluminum foil and placed in front of the light source. ^[b]Suspension / not totally dissolved.

6. Additional NMR Spectra

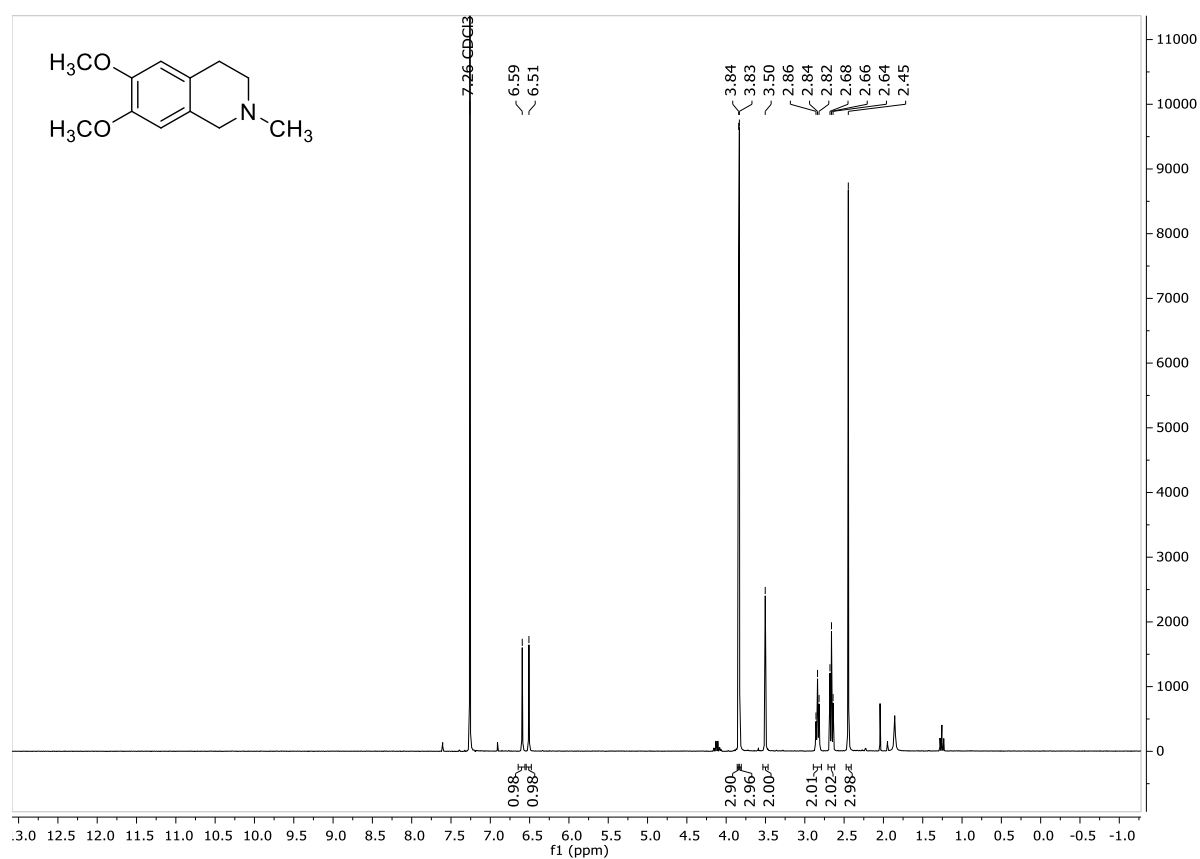


Figure S11. ¹H NMR spectrum (300 MHz, CDCl₃) of 6,7-dimethoxy-2-methyl-1,2,3,4-tetrahydroisoquinoline (**2**).

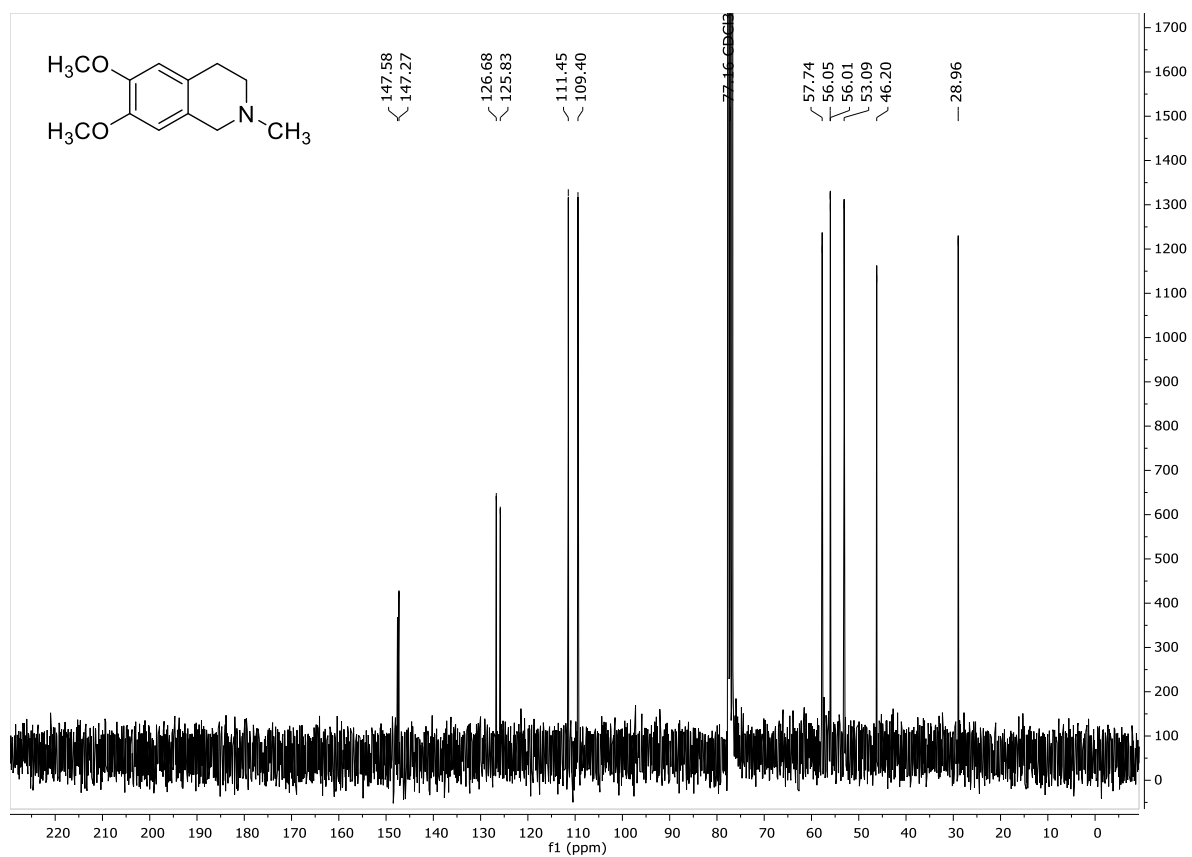


Figure S12. ¹³C NMR spectrum (75 MHz, CDCl₃) of 6,7-dimethoxy-2-methyl-1,2,3,4-tetrahydroisoquinoline (**2**).

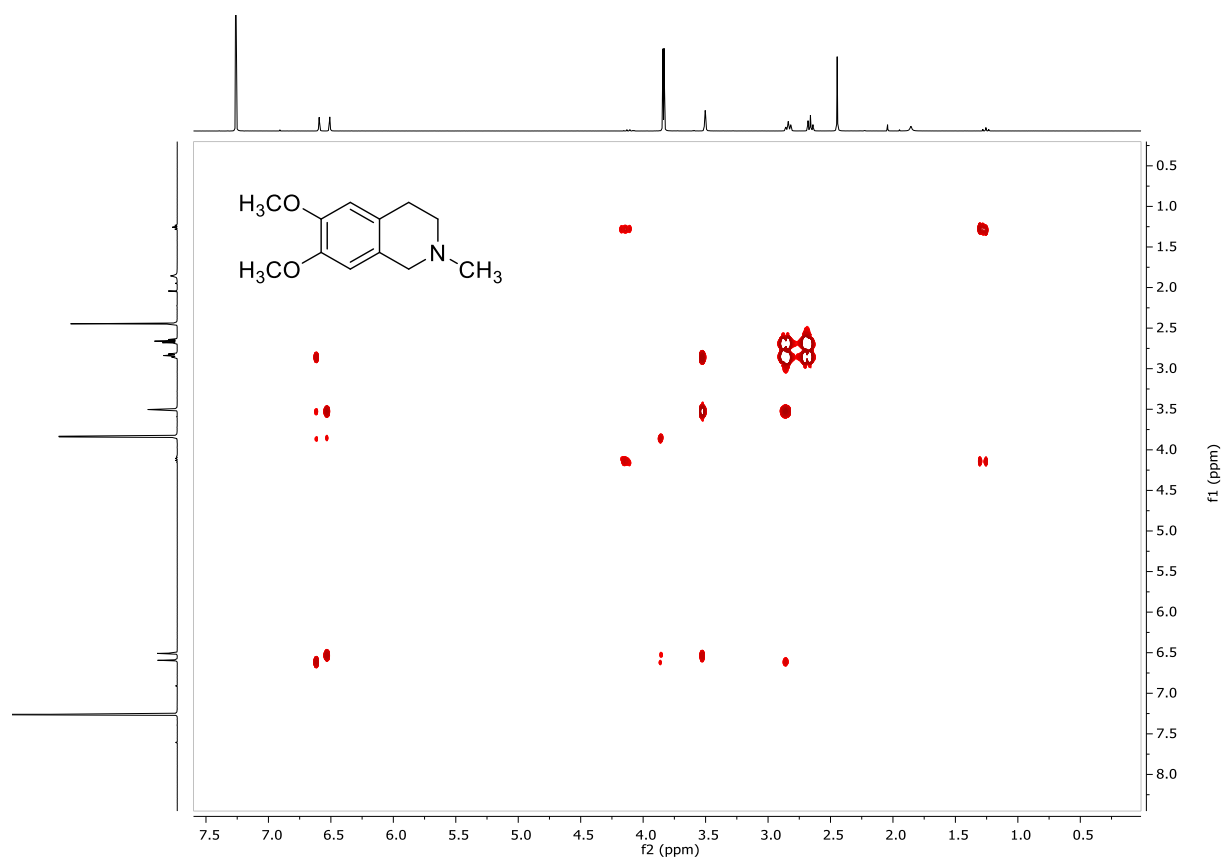


Figure S13. COSY spectrum (CDCl_3) of 6,7-dimethoxy-2-methyl-1,2,3,4-tetrahydroisoquinoline (**2**).

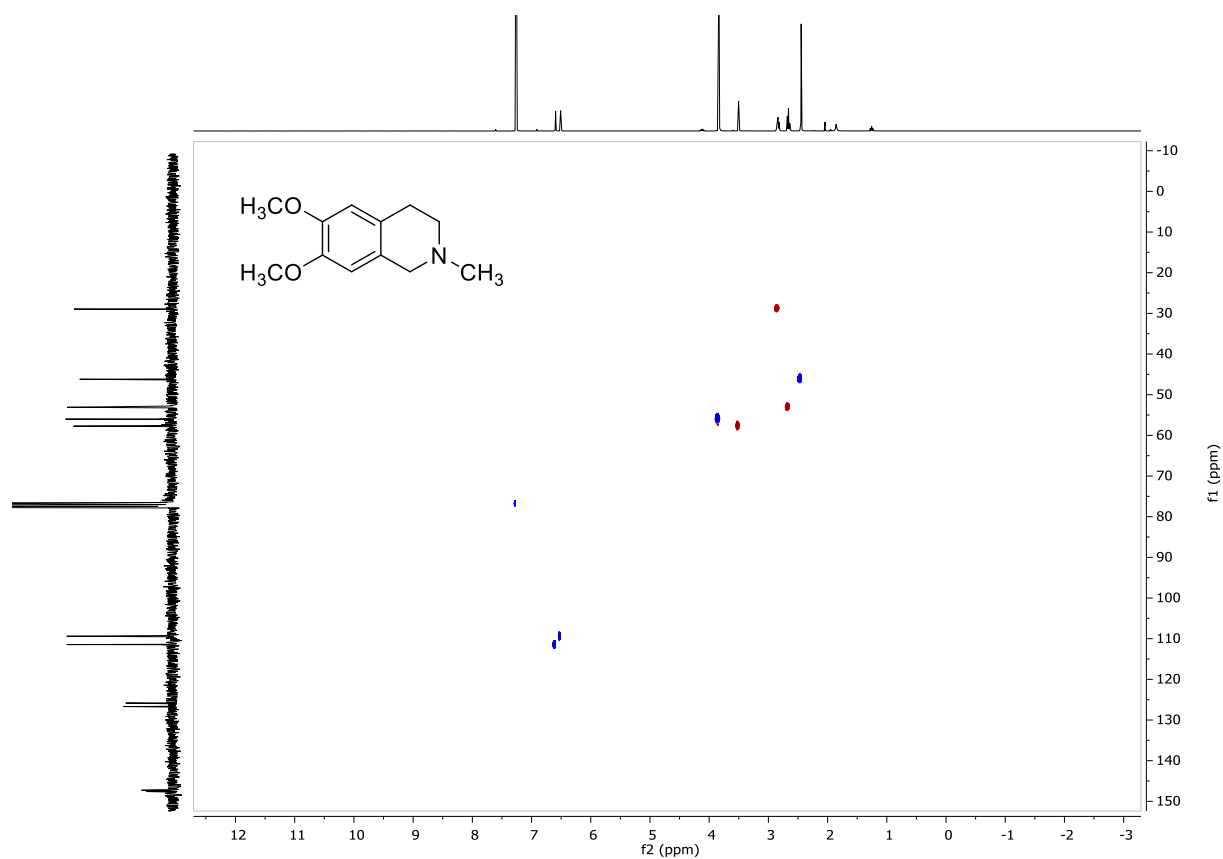


Figure S14. HSQC spectrum (CDCl₃) of 6,7-dimethoxy-2-methyl-1,2,3,4-tetrahydroisoquinoline (**2**).

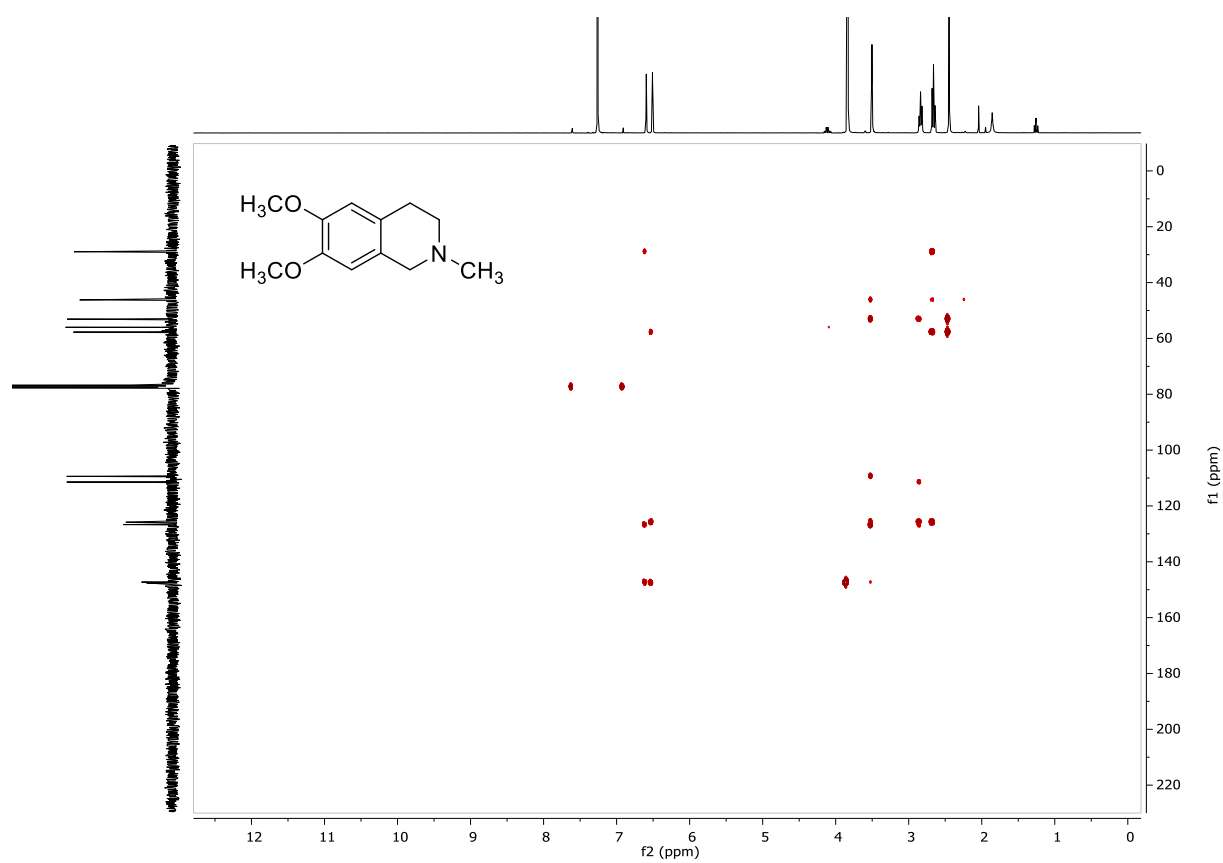


Figure S15. HMBC spectrum (CDCl_3) of 6,7-dimethoxy-2-methyl-1,2,3,4-tetrahydroisoquinoline (**2**).

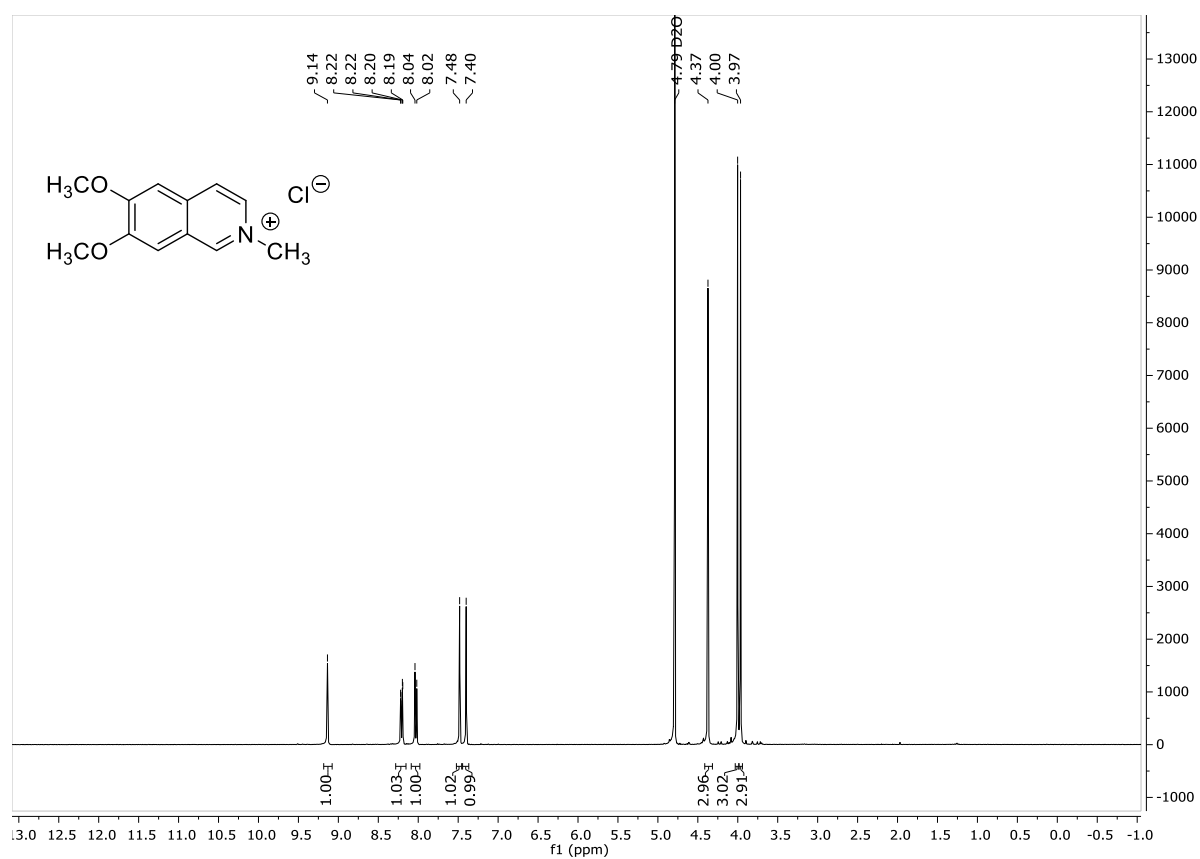


Figure S16. ¹H NMR spectrum (300 MHz, D₂O) of 6,7-dimethoxy-2-methylisoquinolinium chloride (3).

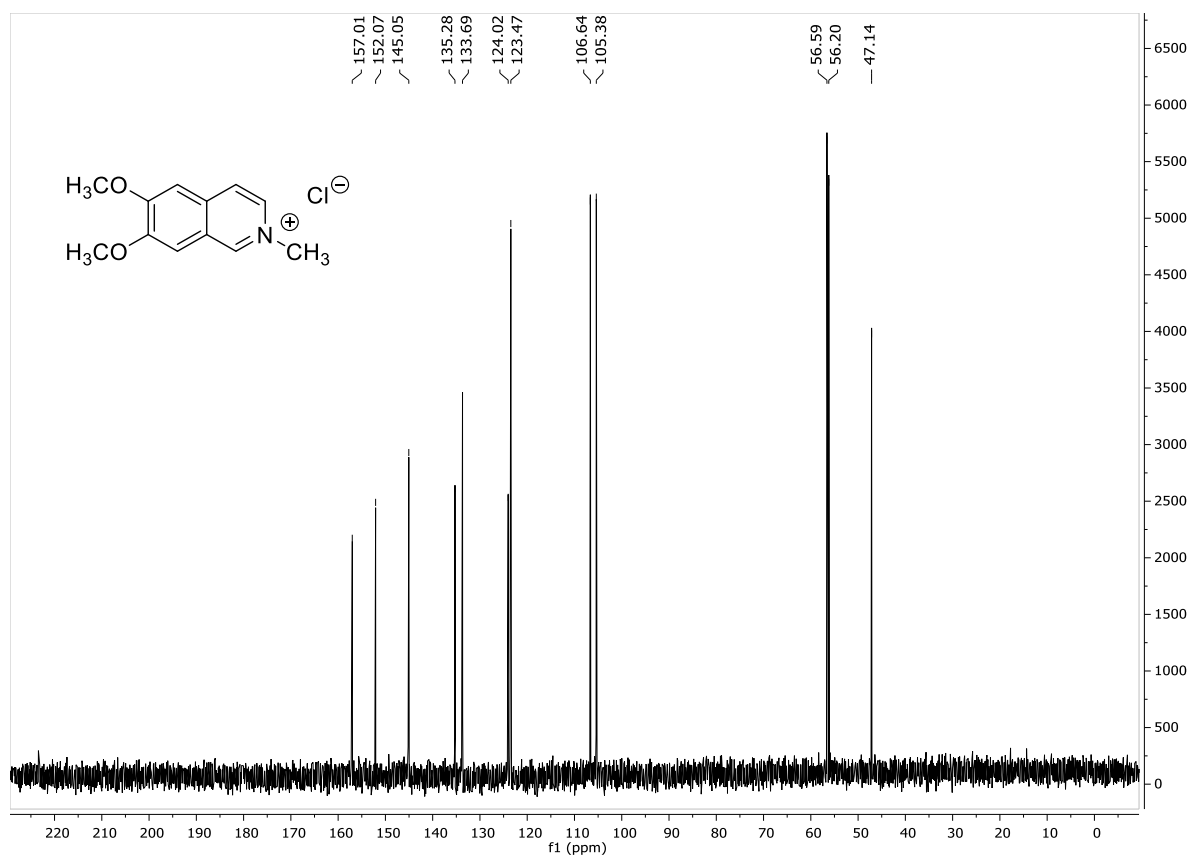


Figure S17. ¹³C NMR spectrum (75 MHz, D₂O) of 6,7-dimethoxy-2-methylisoquinolinium chloride (3).

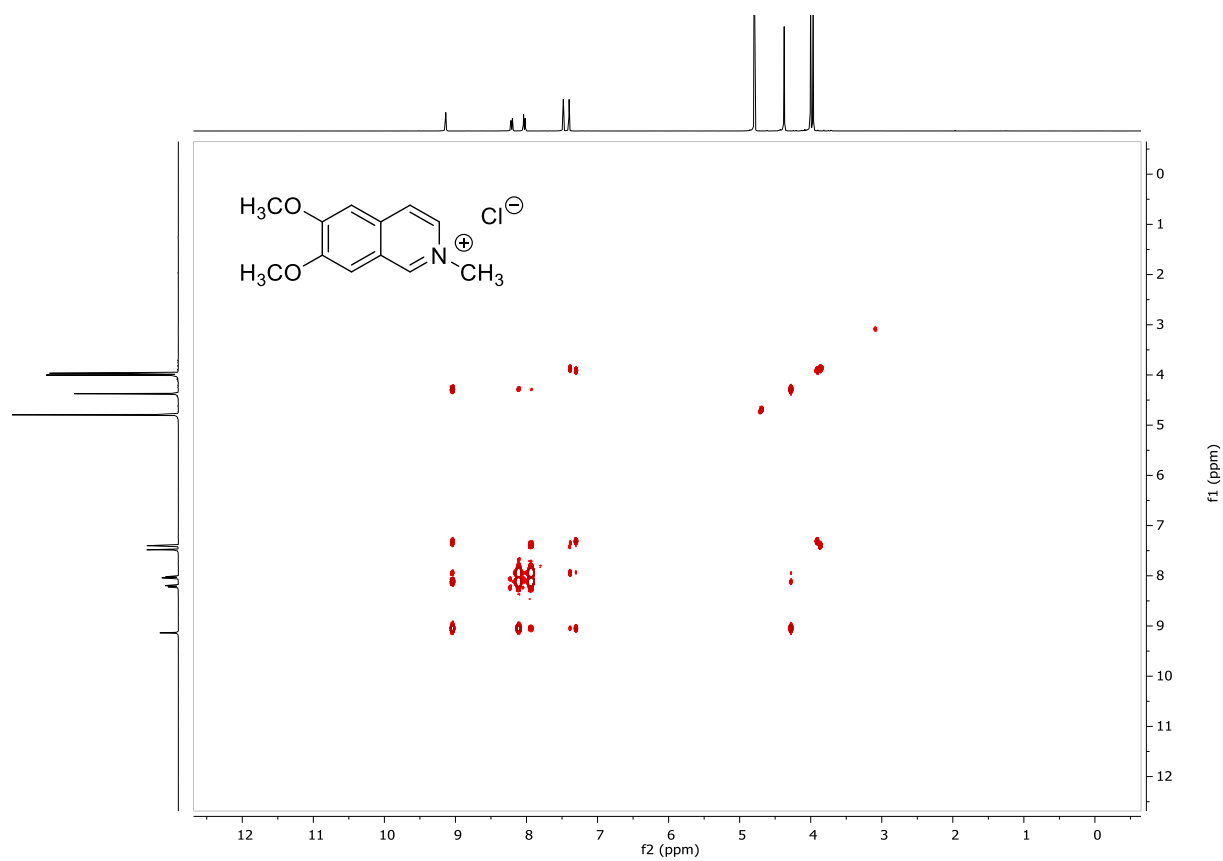


Figure S18. COSY spectrum (D_2O) of 6,7-dimethoxy-2-methylisoquinolinium chloride (**3**).

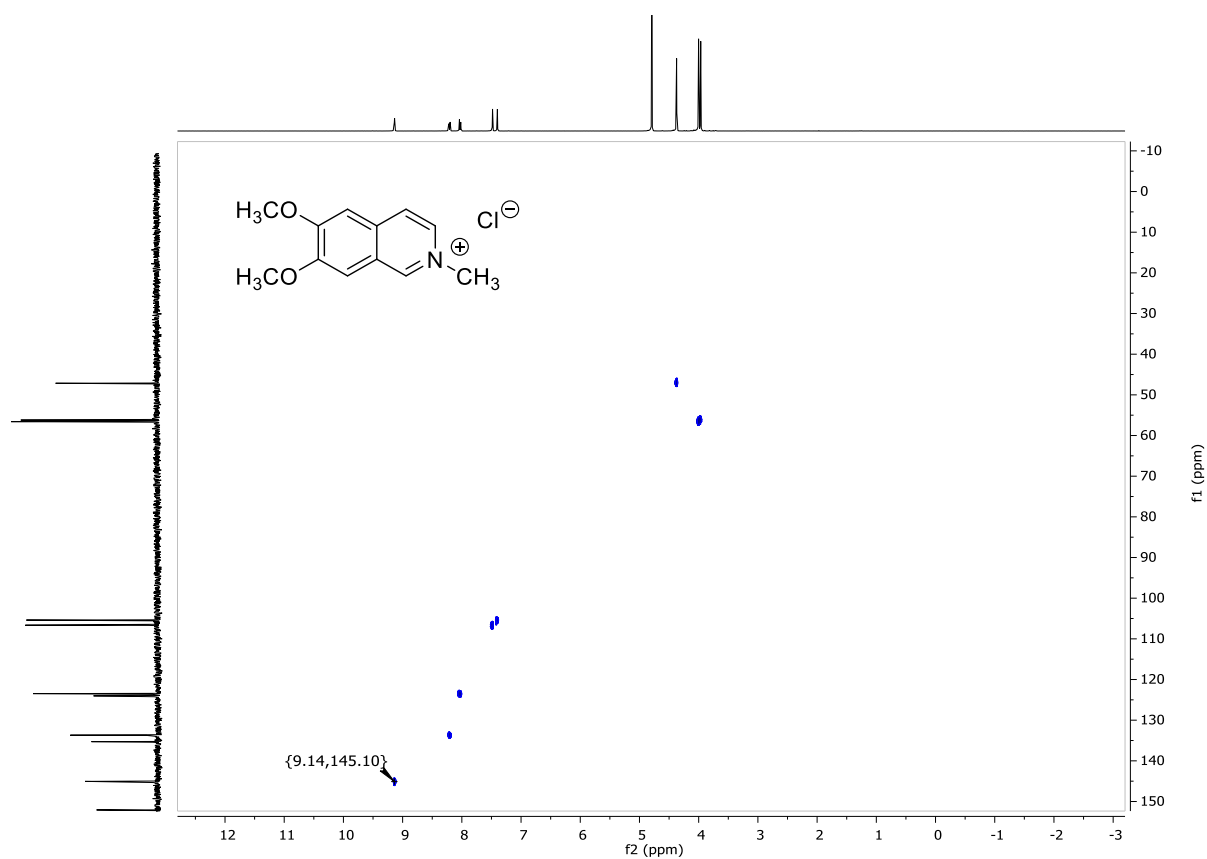


Figure S19. HSQC spectrum (D₂O) of 6,7-dimethoxy-2-methylisoquinolinium chloride (**3**).

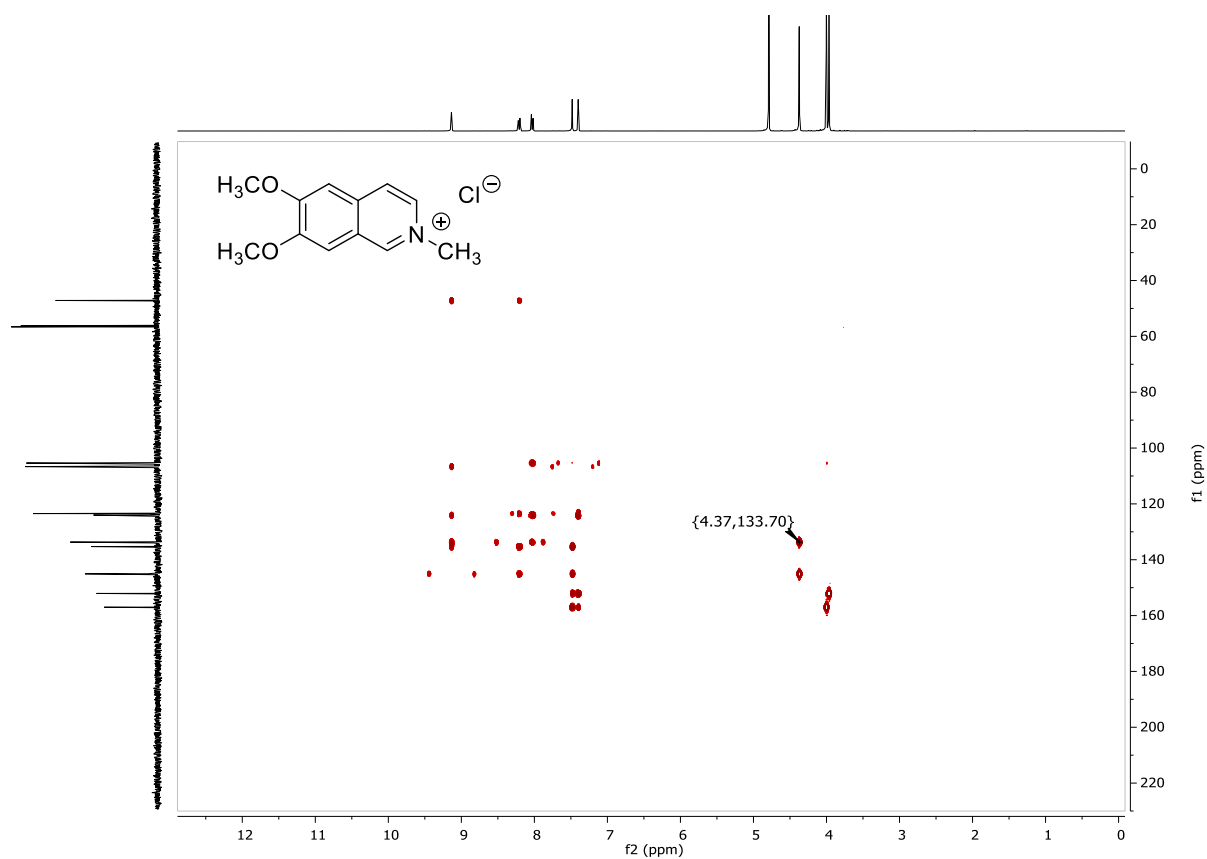


Figure S20. HMBC spectrum (D₂O) of 6,7-dimethoxy-2-methylisoquinolinium chloride (**3**).

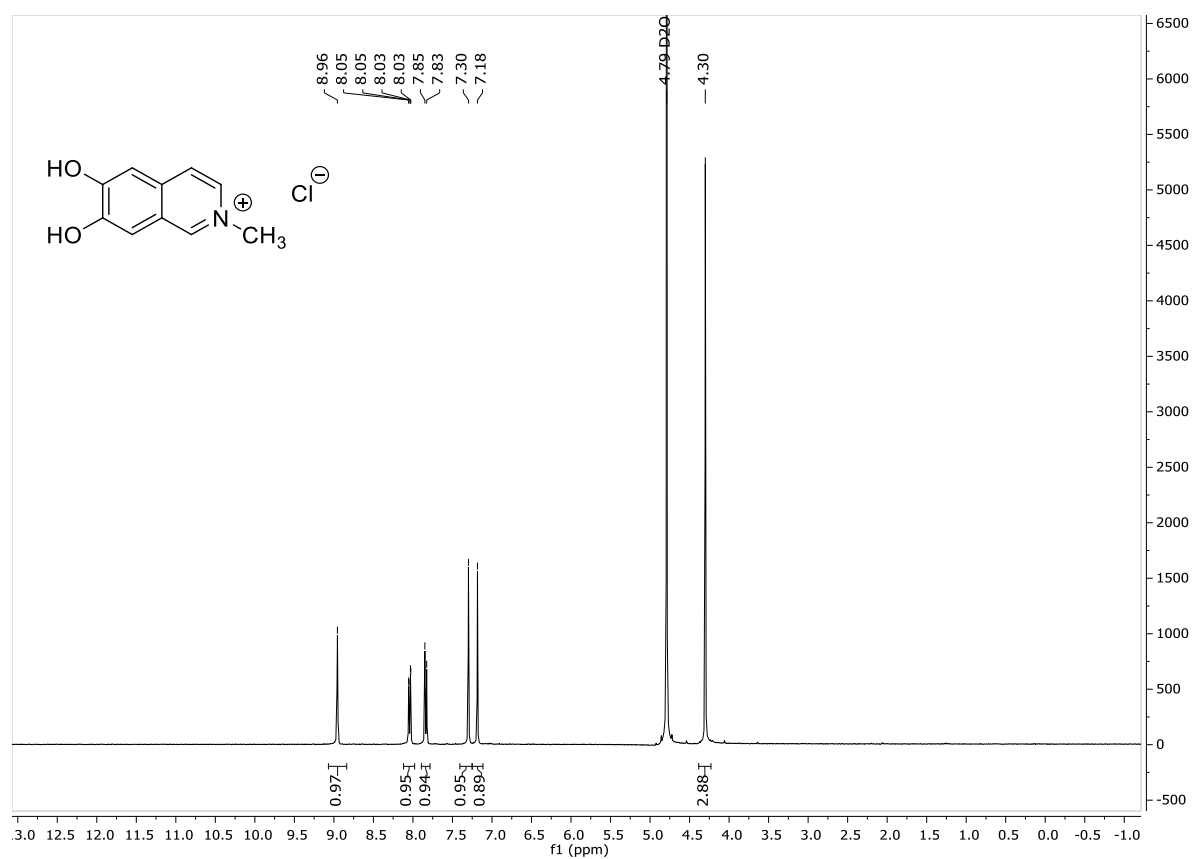


Figure S21. ¹H NMR spectrum (300 MHz, D₂O) of 6,7-dihydroxy-2-methylisoquinolinium chloride (DHMIQ).

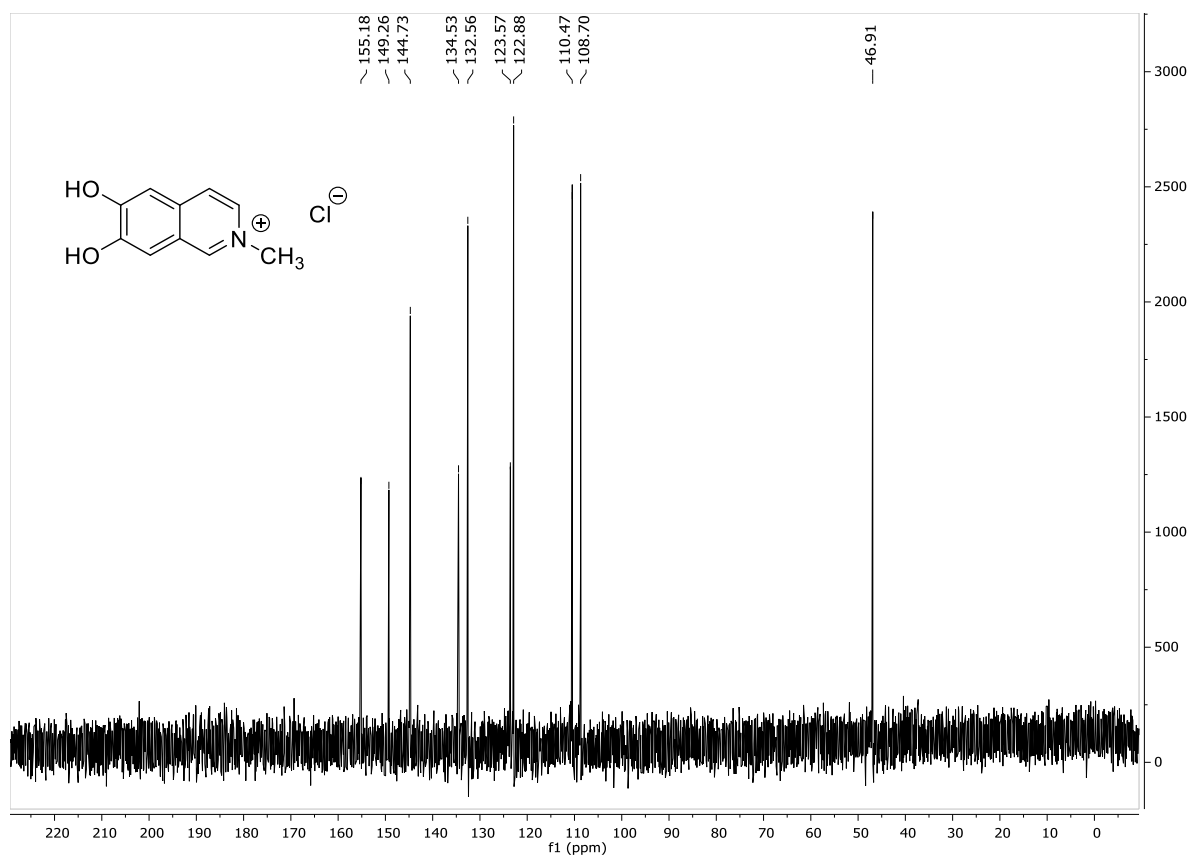


Figure S22. ^{13}C NMR spectrum (75 MHz, D_2O) of 6,7-dihydroxy-2-methylisoquinolinium chloride (DHMIQ).

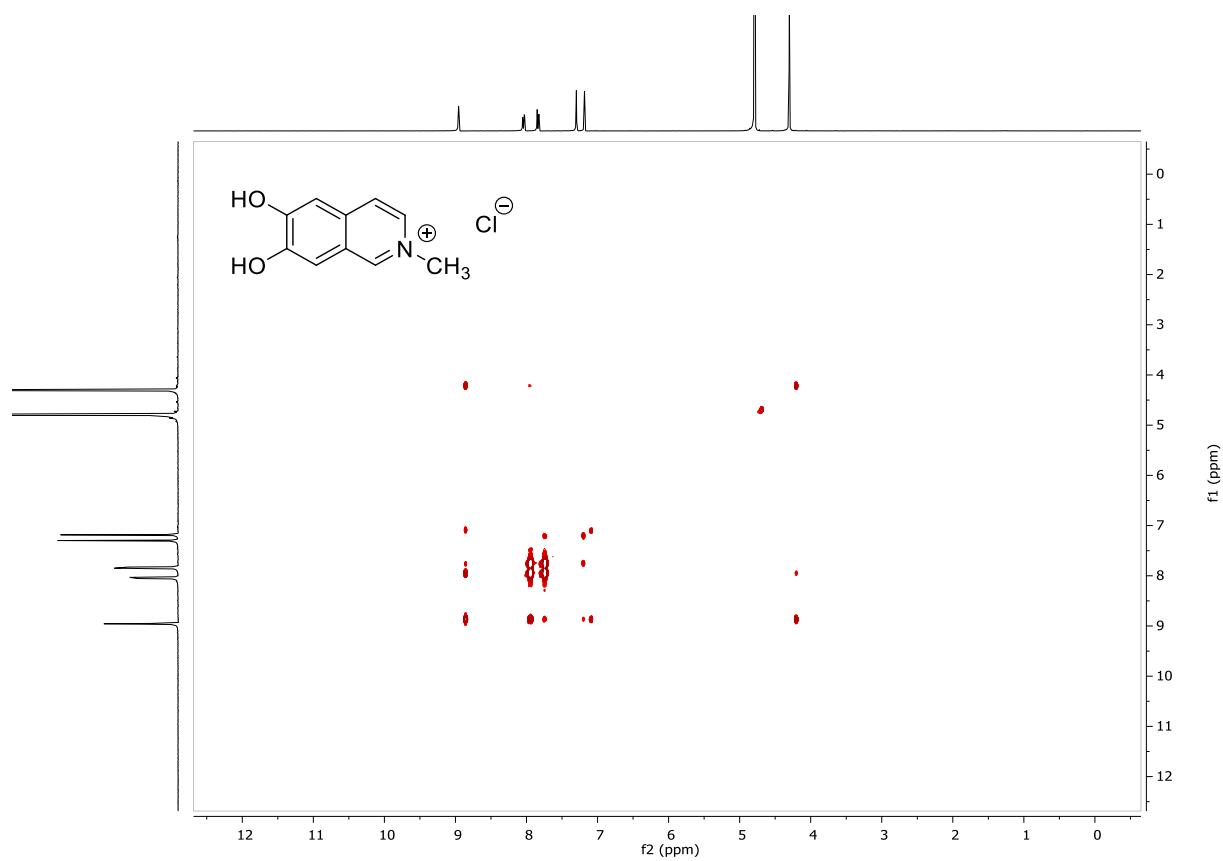


Figure S23. COSY spectrum (D₂O) of 6,7-dihydroxy-2-methylisoquinolinium chloride (DHMIQ).

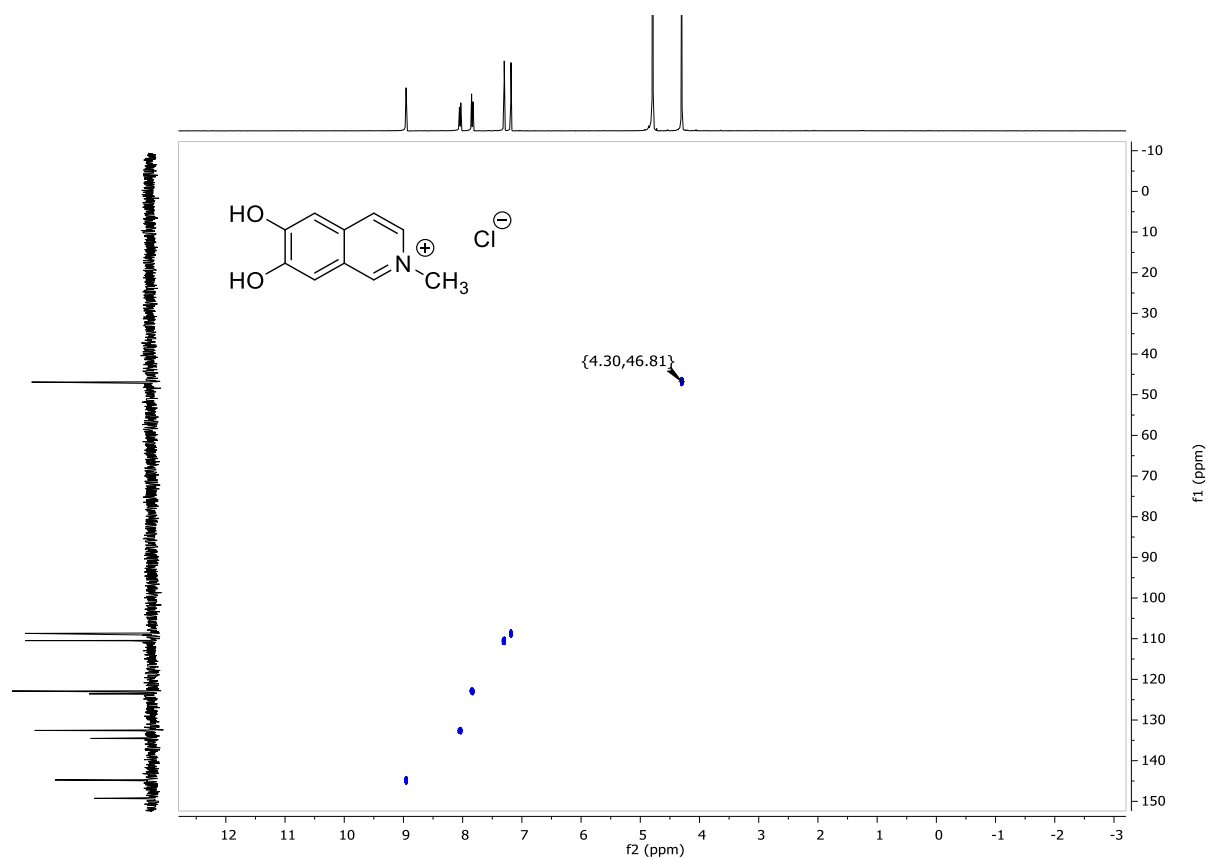


Figure S24. HSQC spectrum (D₂O) of 6,7-dihydroxy-2-methylisoquinolinium chloride (DHMIQ).

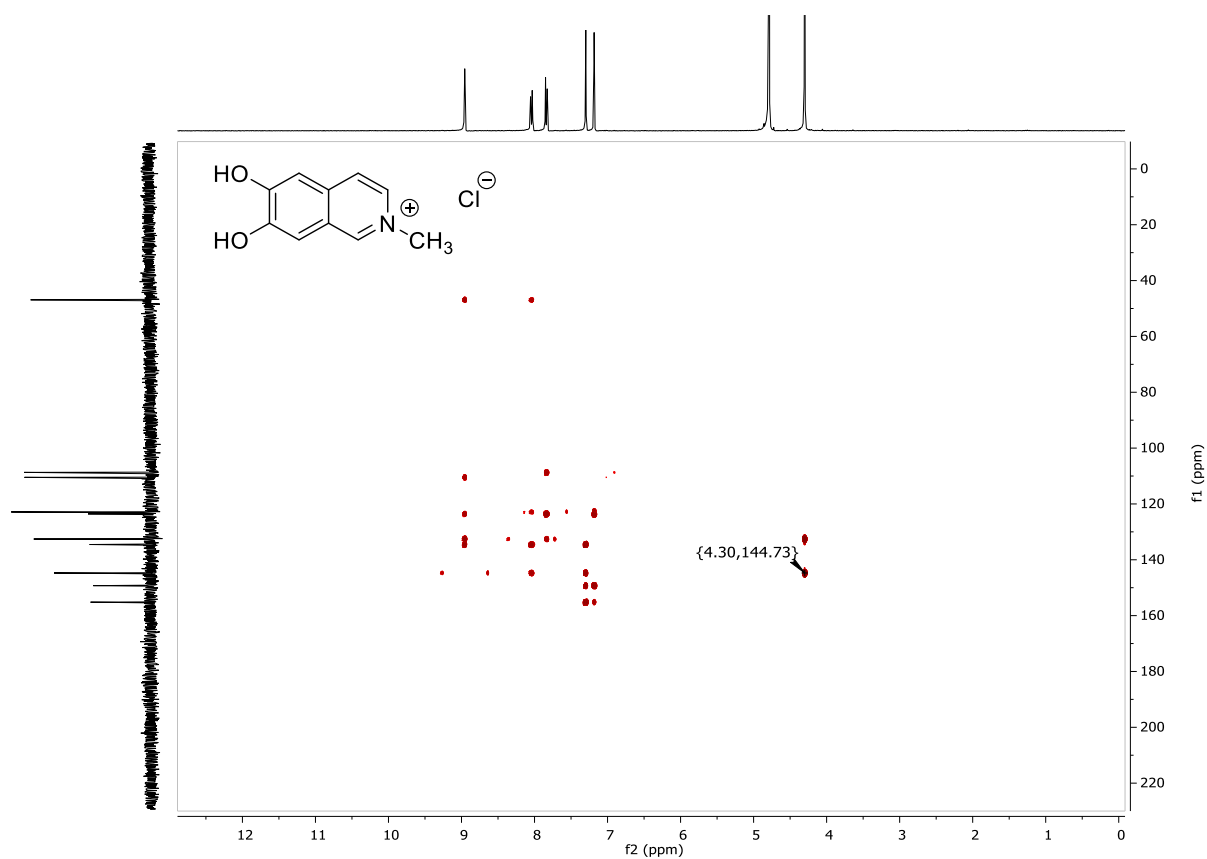


Figure S25. HMBC spectrum (D_2O) of 6,7-dihydroxy-2-methylisoquinolinium chloride (DHMIQ).

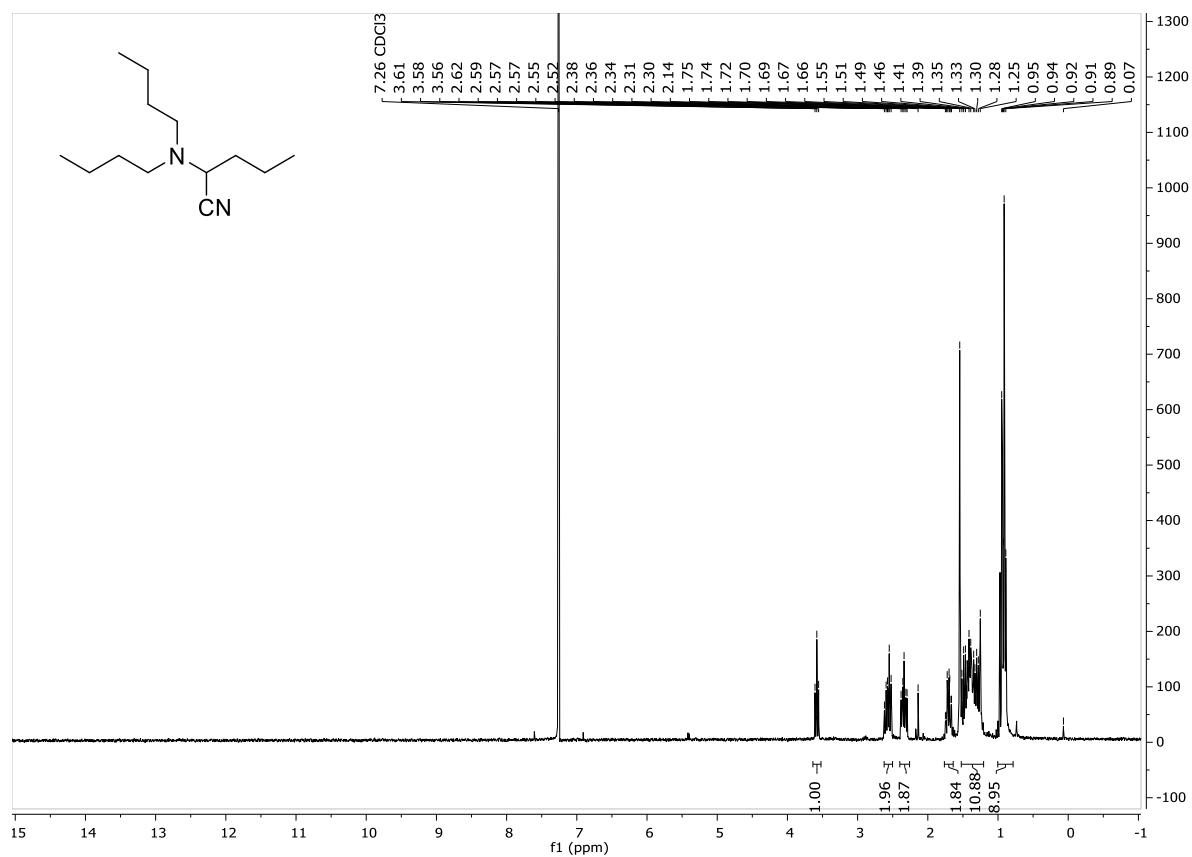


Figure S26. ¹H NMR spectrum (300 MHz, CDCl₃) of 2-(dibutylamino)-pentanenitrile (**5**).

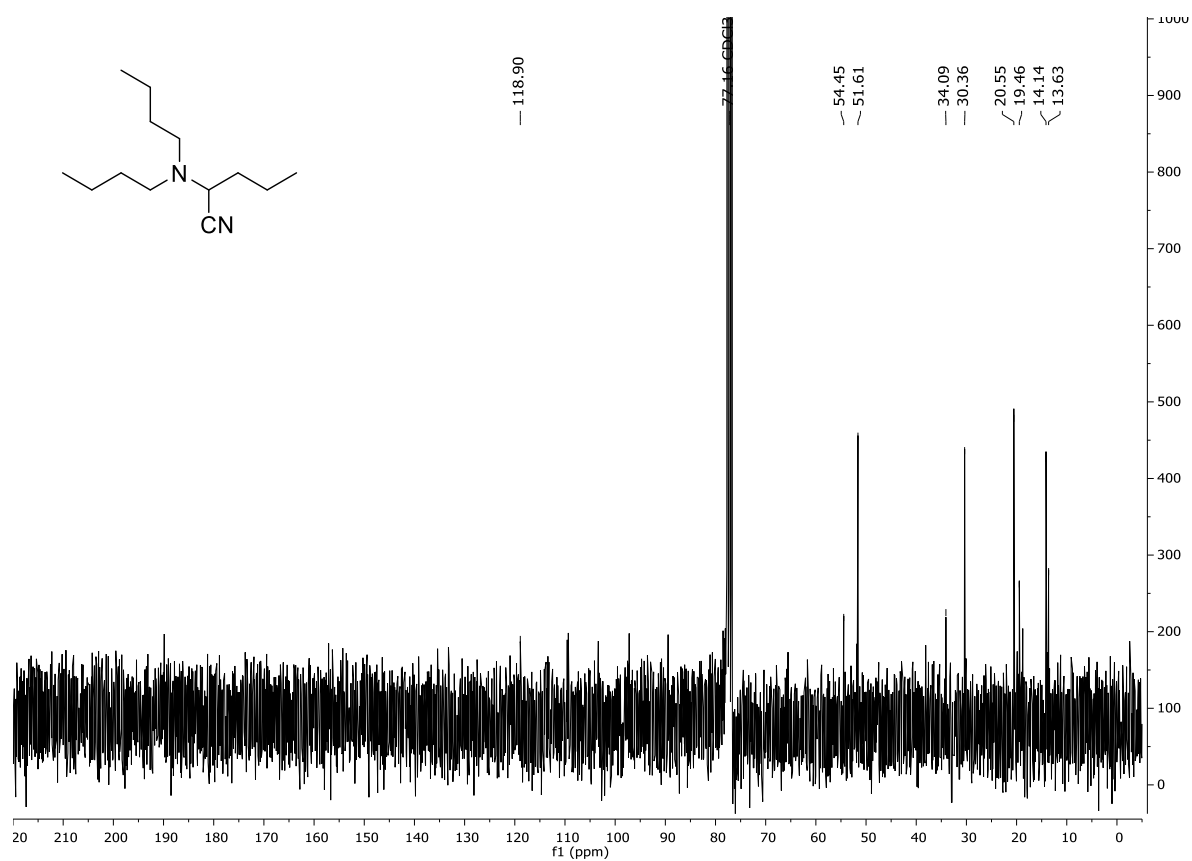


Figure S27. ¹³C NMR spectrum (75 MHz, CDCl₃) of 2-(dibutylamino)-pentanenitrile (**5**). The CN-signal (118.9 ppm) was determined by HMBC.

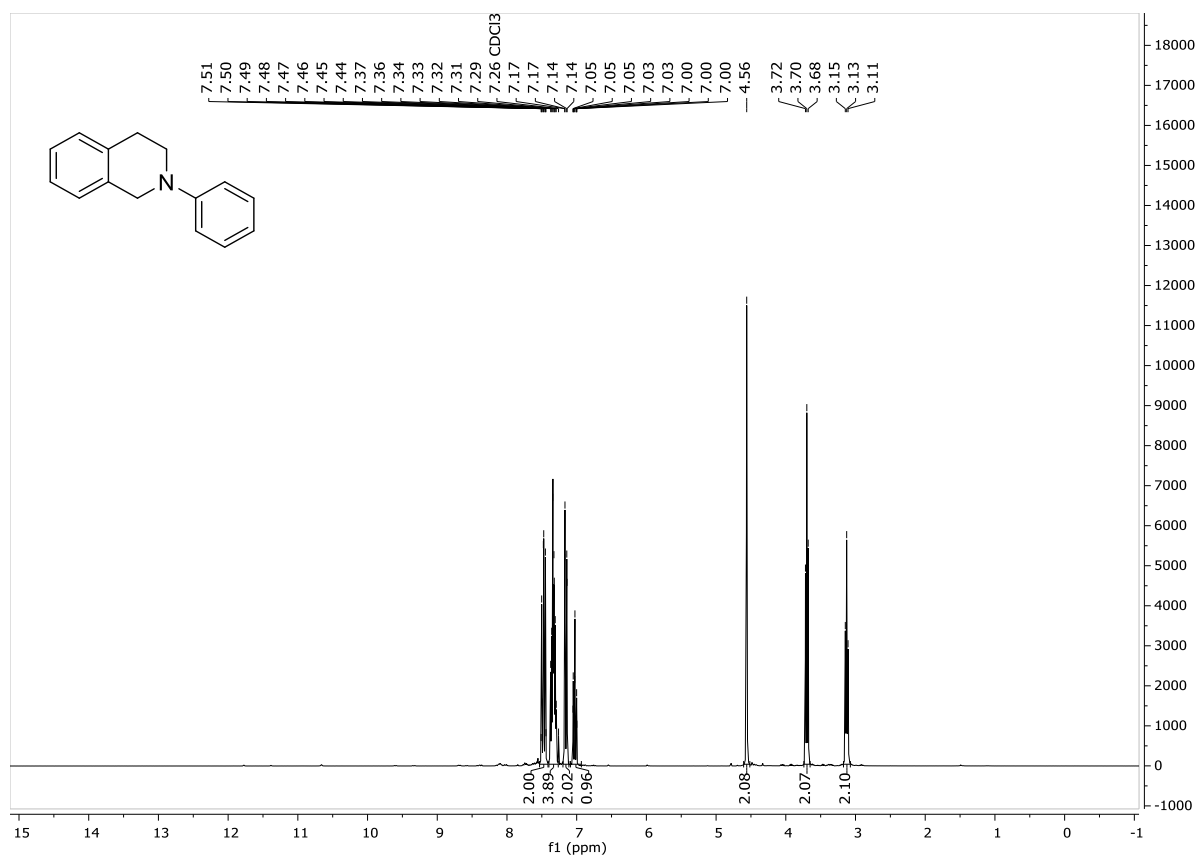


Figure S28. ¹H NMR spectrum (300 MHz, CDCl₃) of *N*-phenyl-1,2,3,4-tetrahydroisoquinoline (6).

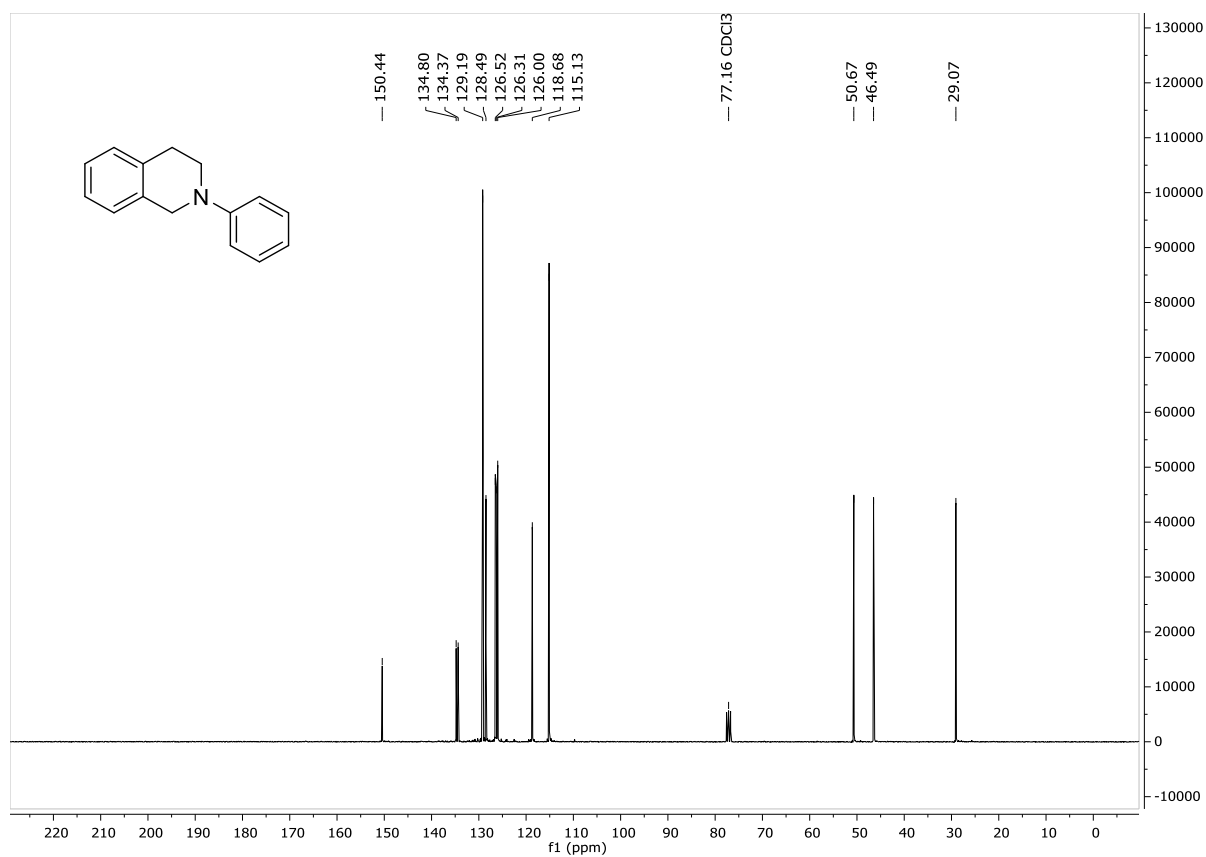


Figure S29. ^{13}C NMR spectrum (75 MHz, CDCl_3) of *N*-phenyl-1,2,3,4-tetrahydroisoquinoline (6).

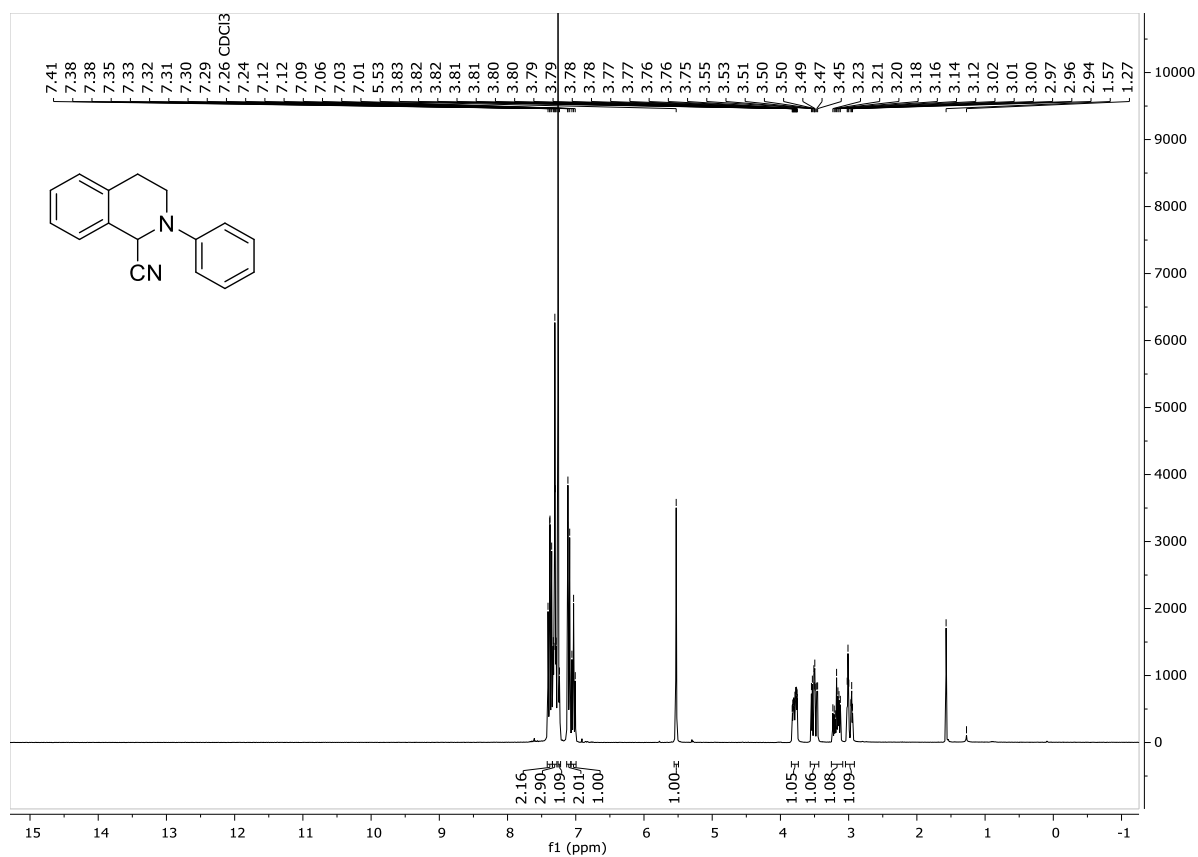


Figure S30. ¹H NMR spectrum (300 MHz, CDCl₃) of *N*-phenyl-1,2,3,4-tetrahydroisoquinoline-1-carbonitrile (14).

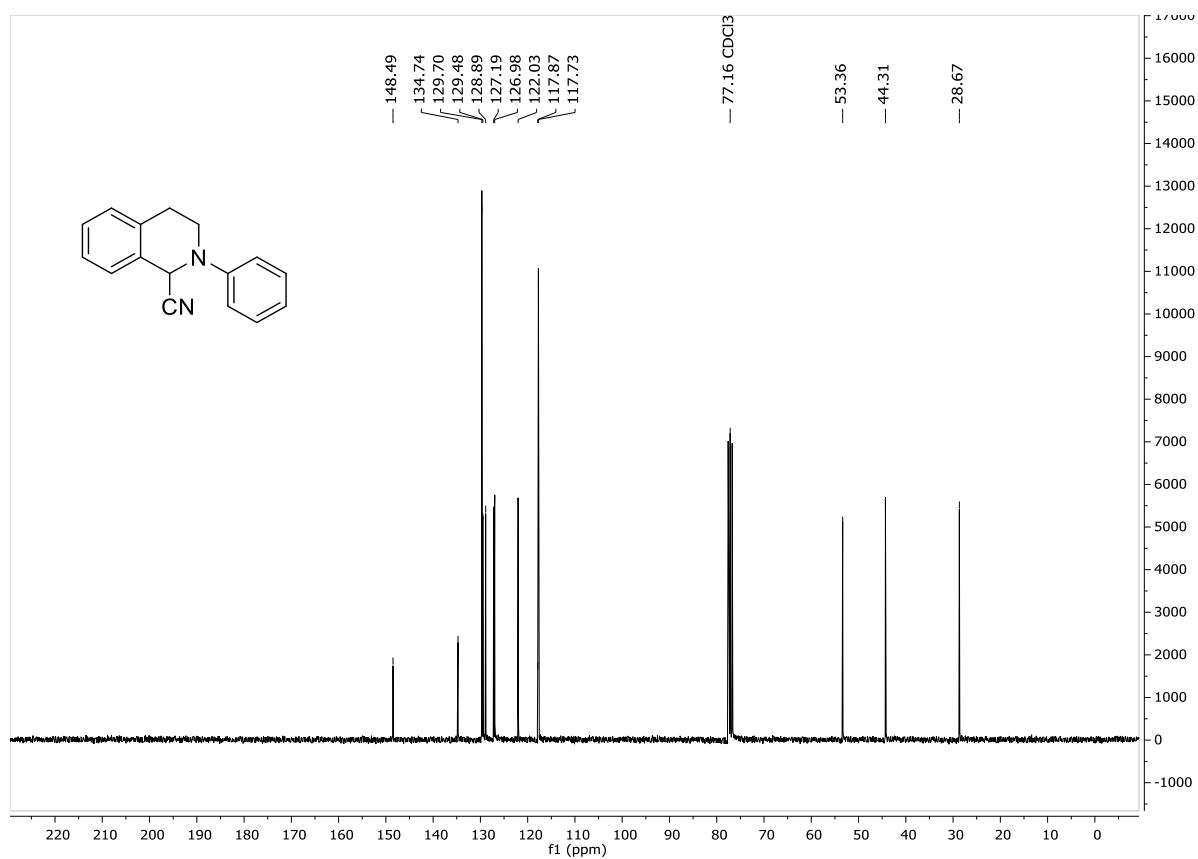


Figure S31. ¹³C NMR spectrum (75 MHz, CDCl₃) of *N*-phenyl-1,2,3,4-tetrahydroisoquinoline-1-carbonitrile (**14**).

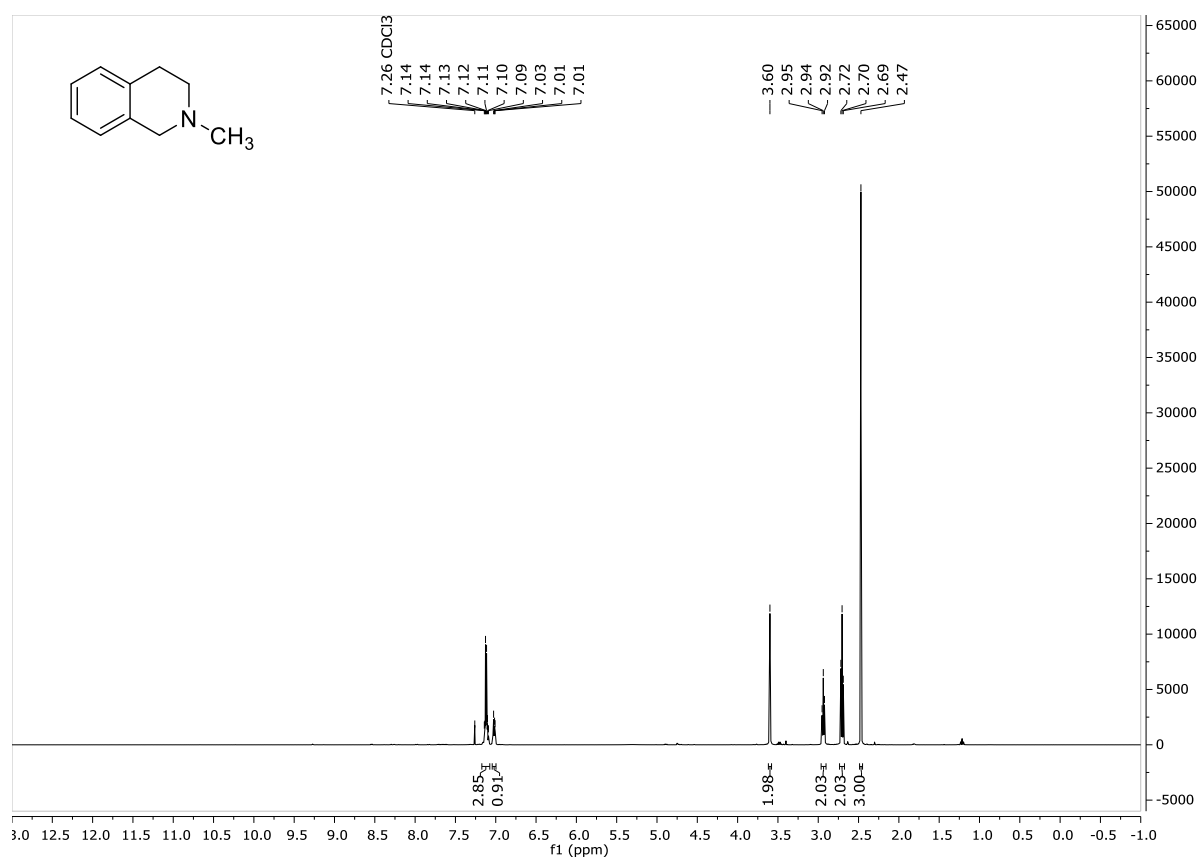


Figure S32. ¹H NMR spectrum (300 MHz, CDCl₃) of *N*-methyl-1,2,3,4-tetrahydroisoquinoline (7).

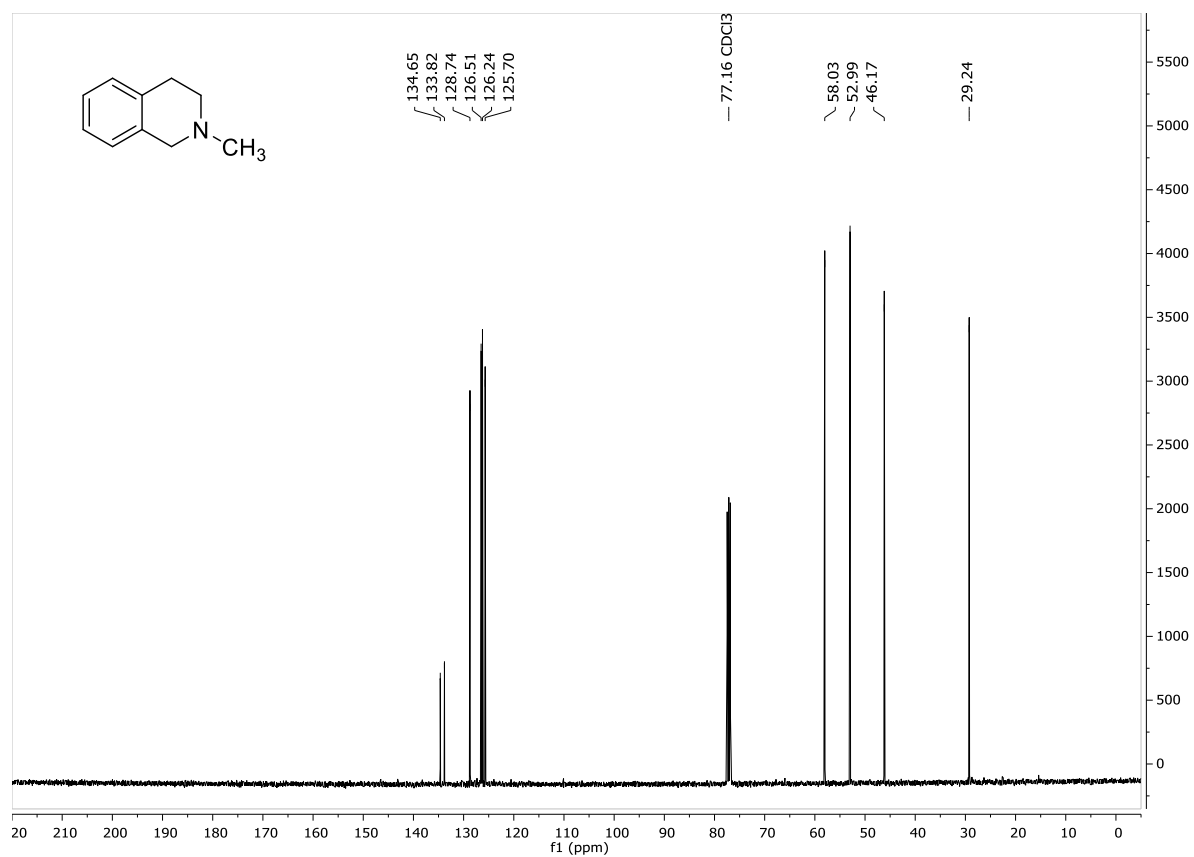


Figure S33. ¹³C NMR spectrum (75 MHz, CDCl₃) of *N*-methyl-1,2,3,4-tetrahydroisoquinoline (7).

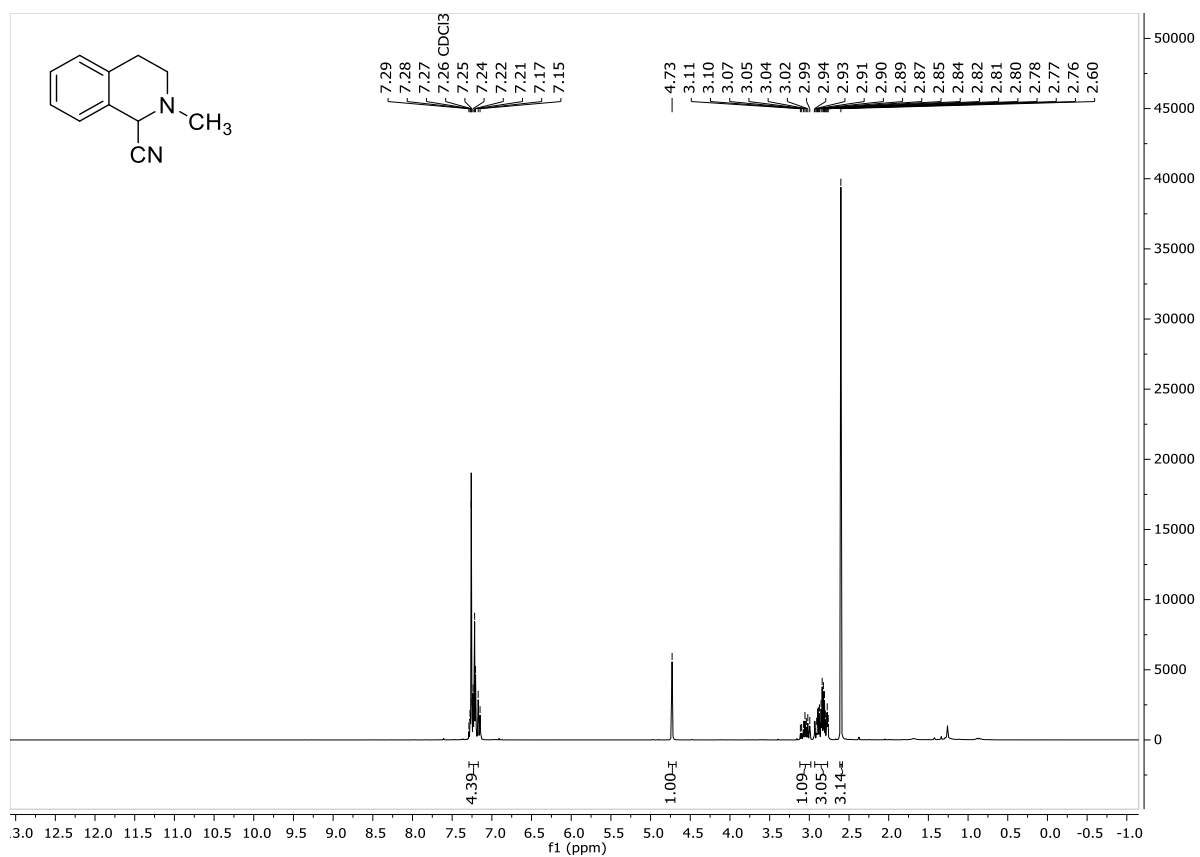


Figure S34. ¹H NMR spectrum (300 MHz, CDCl₃) of *N*-methyl-1,2,3,4-tetrahydroisoquinoline-1-carbonitrile (**15**).

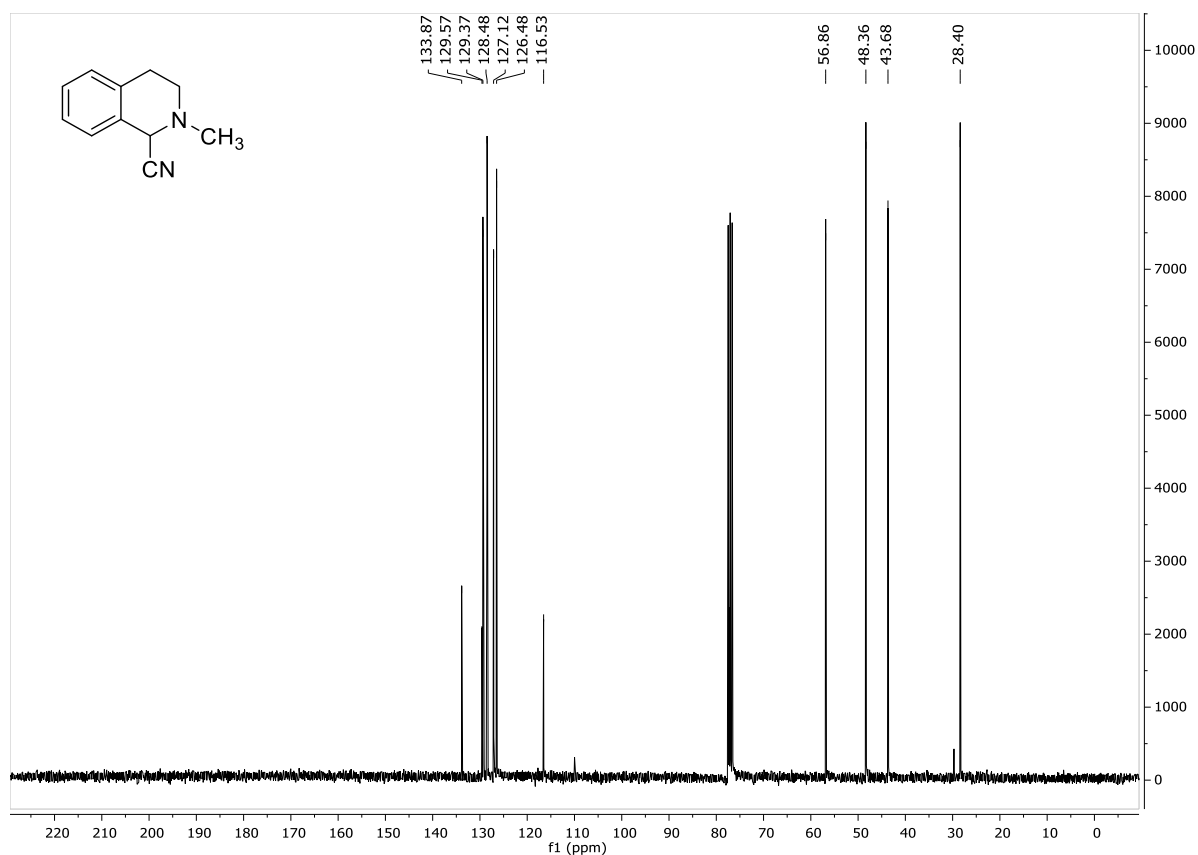


Figure S35. ^{13}C NMR spectrum (75 MHz, CDCl_3) of *N*-methyl-1,2,3,4-tetrahydroisoquinoline-1-carbonitrile (**15**).

NOTE: The α -aminonitriles derived from trialkylamines are prone to the slow elimination of HCN which may lead to baseline clutter in the respective NMR spectra. This behavior correlates with the electron density at nitrogen and the stabilization of the iminium ion/enamine formed.

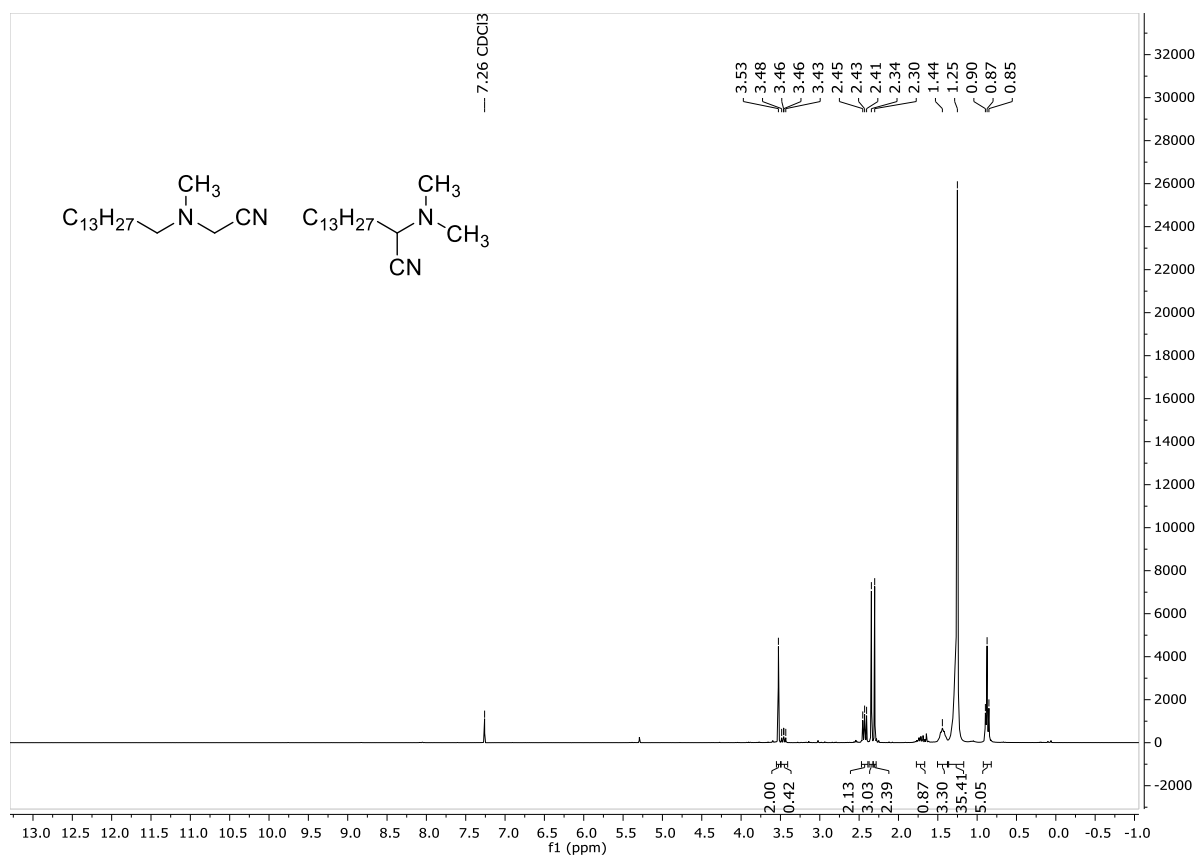


Figure S36. ¹H NMR spectrum (300 MHz, CDCl₃) of the mixture of [tetradecyl(methyl)amino]-acetonitrile (**16**) and 2-(dimethylamino)pentadecanenitrile (**17**).

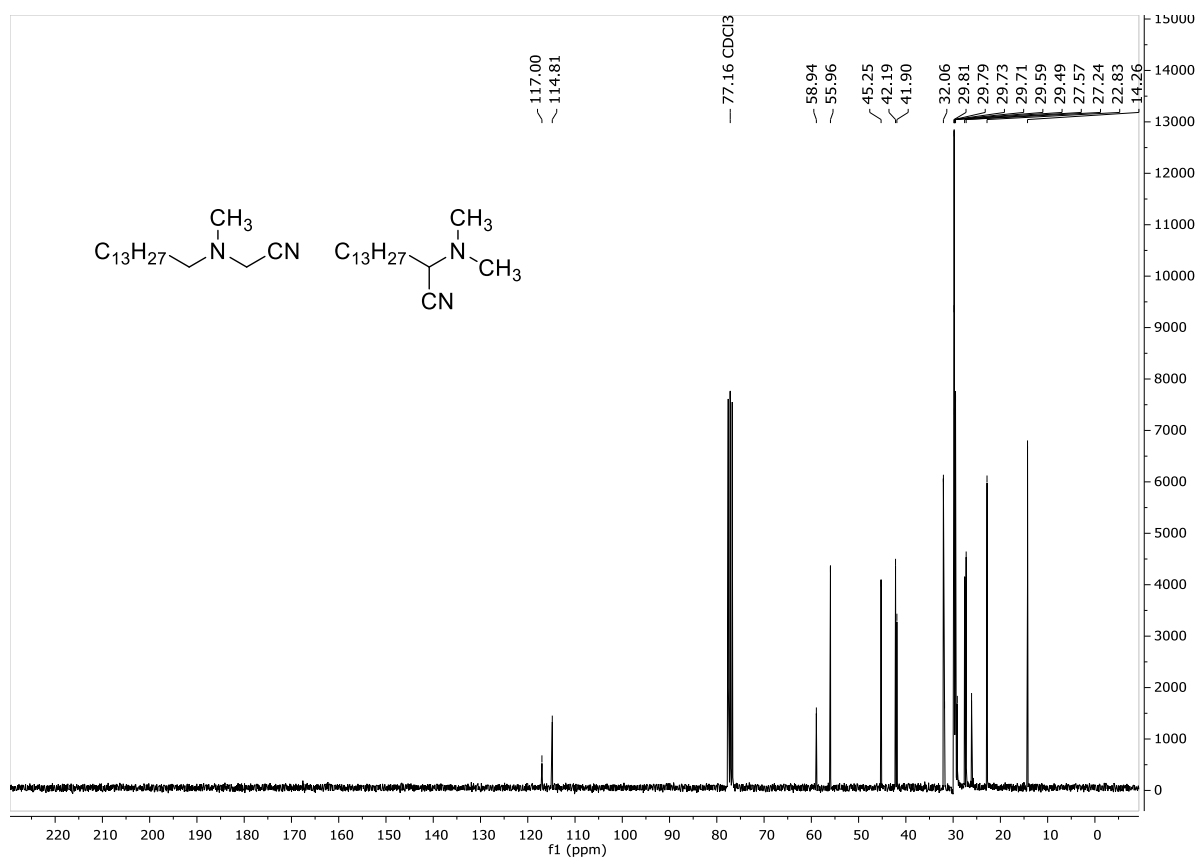


Figure S37. ^{13}C NMR spectrum (75 MHz, CDCl_3) of the mixture of [tetradecyl(methyl)amino]-acetonitrile (**16**) and 2-(dimethylamino)pentadecanenitrile (**17**).

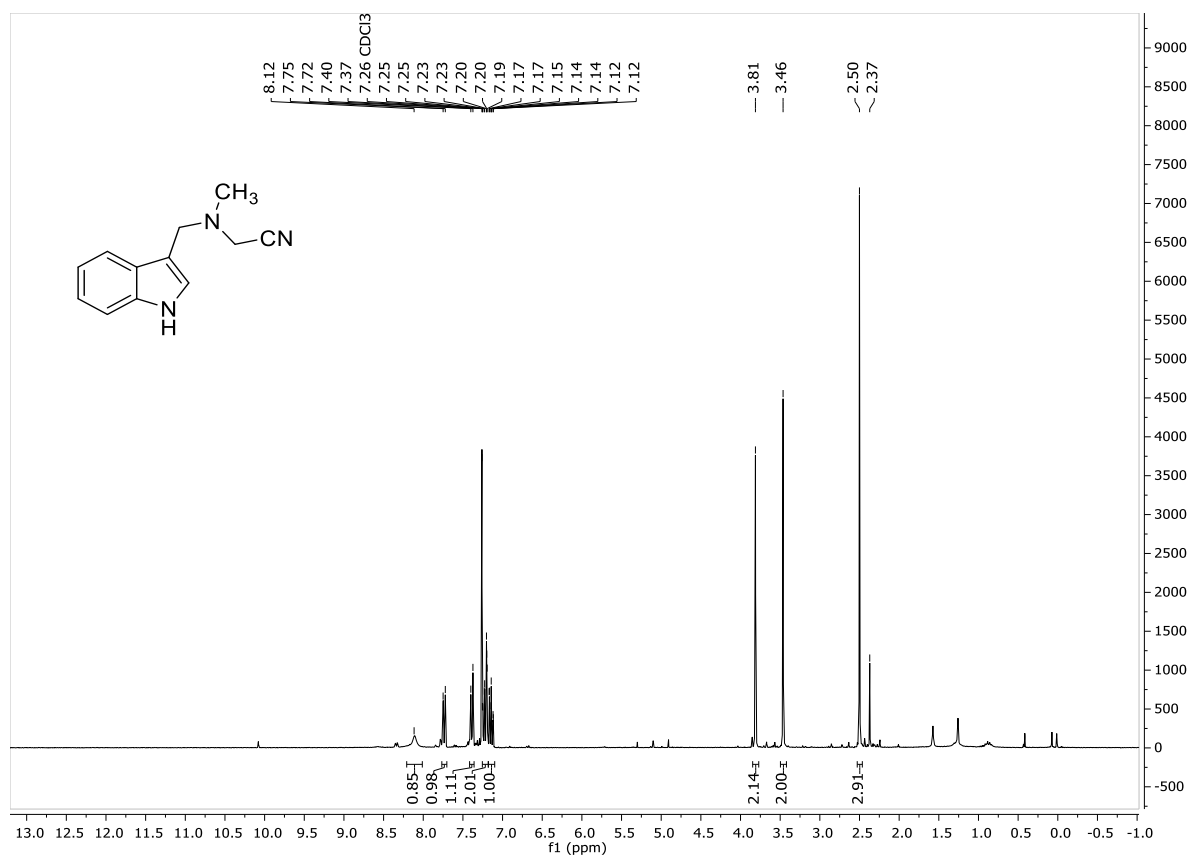


Figure S38. ¹H NMR spectrum (300 MHz, CDCl₃) of [(1*H*-indol-3-ylmethyl)(methyl)amino]-acetonitrile (**18**).

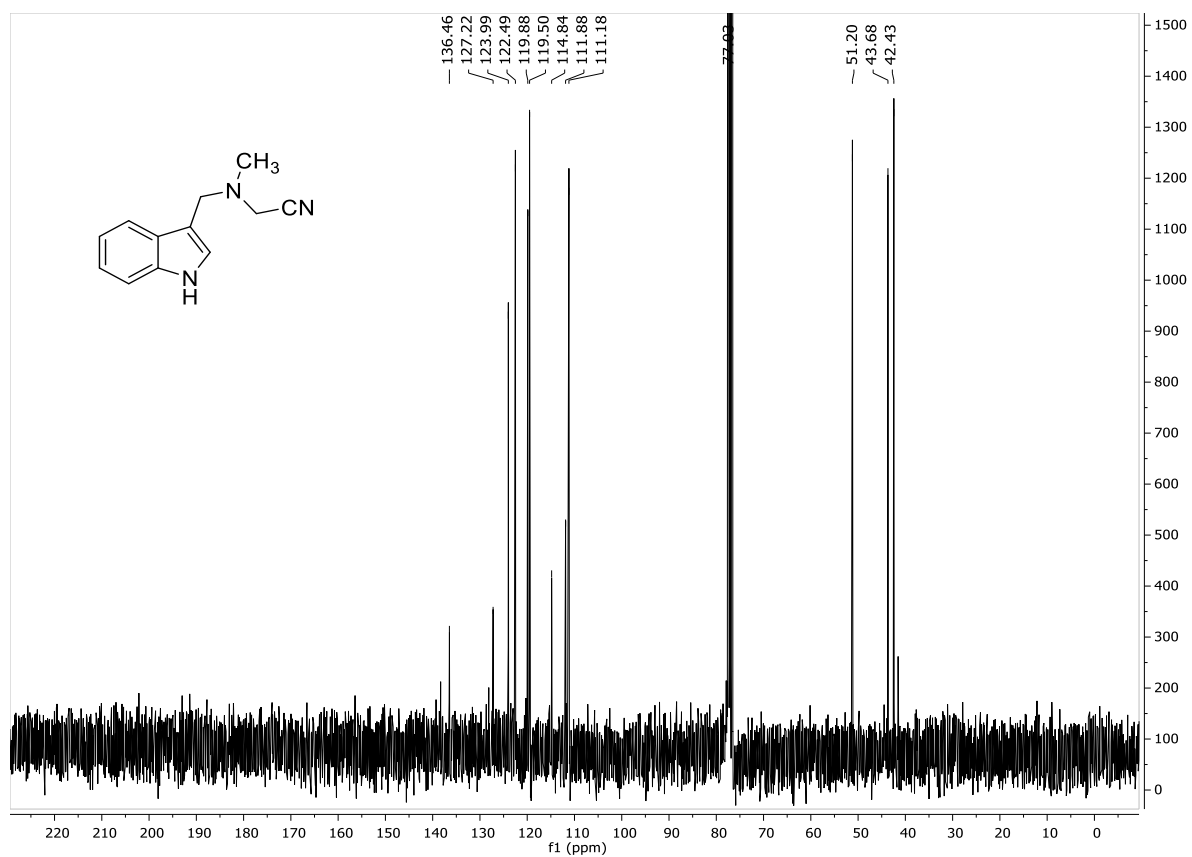


Figure S39. ¹³C NMR spectrum (75 MHz, CDCl₃) of [(1*H*-indol-3-ylmethyl)(methyl)amino]-acetonitrile (**18**).

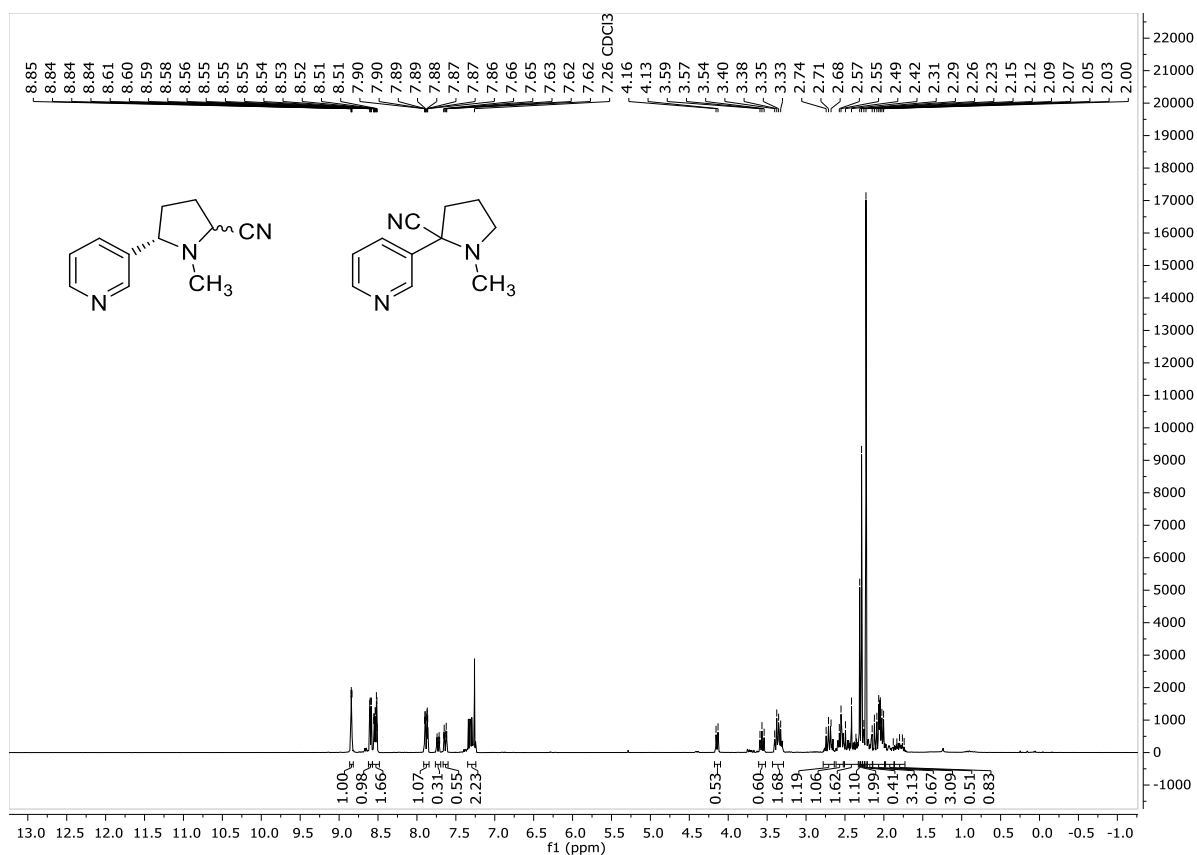


Figure S40. ^1H NMR spectrum (300 MHz, CDCl_3) of the mixture of 1-methyl-5-(pyridin-3-yl)pyrrolidine-2-carbonitrile (19) and 1-methyl-2-(pyridin-3-yl)pyrrolidine-2-carbonitrile (20).

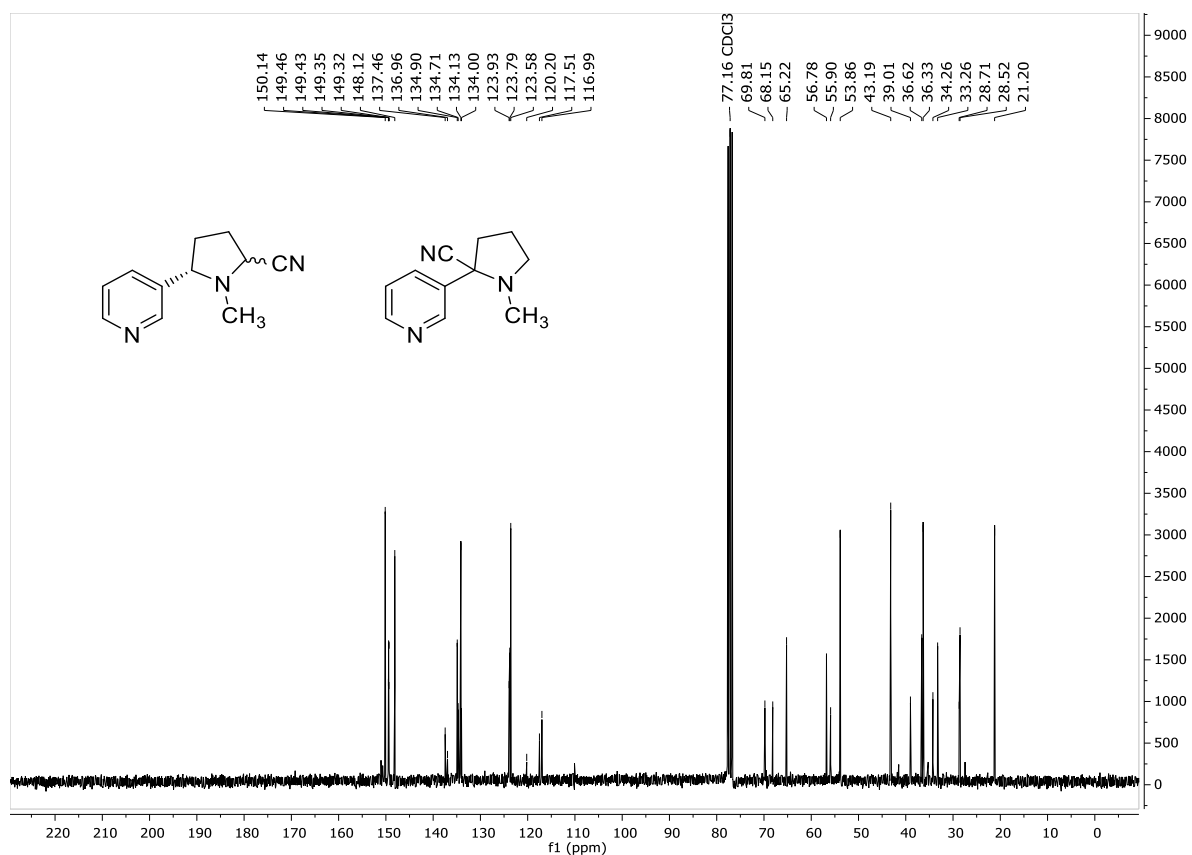


Figure S41. ¹³C NMR spectrum (75 MHz, CDCl₃) of the mixture of 1-methyl-5-(pyridin-3-yl)pyrrolidine-2-carbonitrile (**19**) and 1-methyl-2-(pyridin-3-yl)pyrrolidine-2-carbonitrile (**20**).

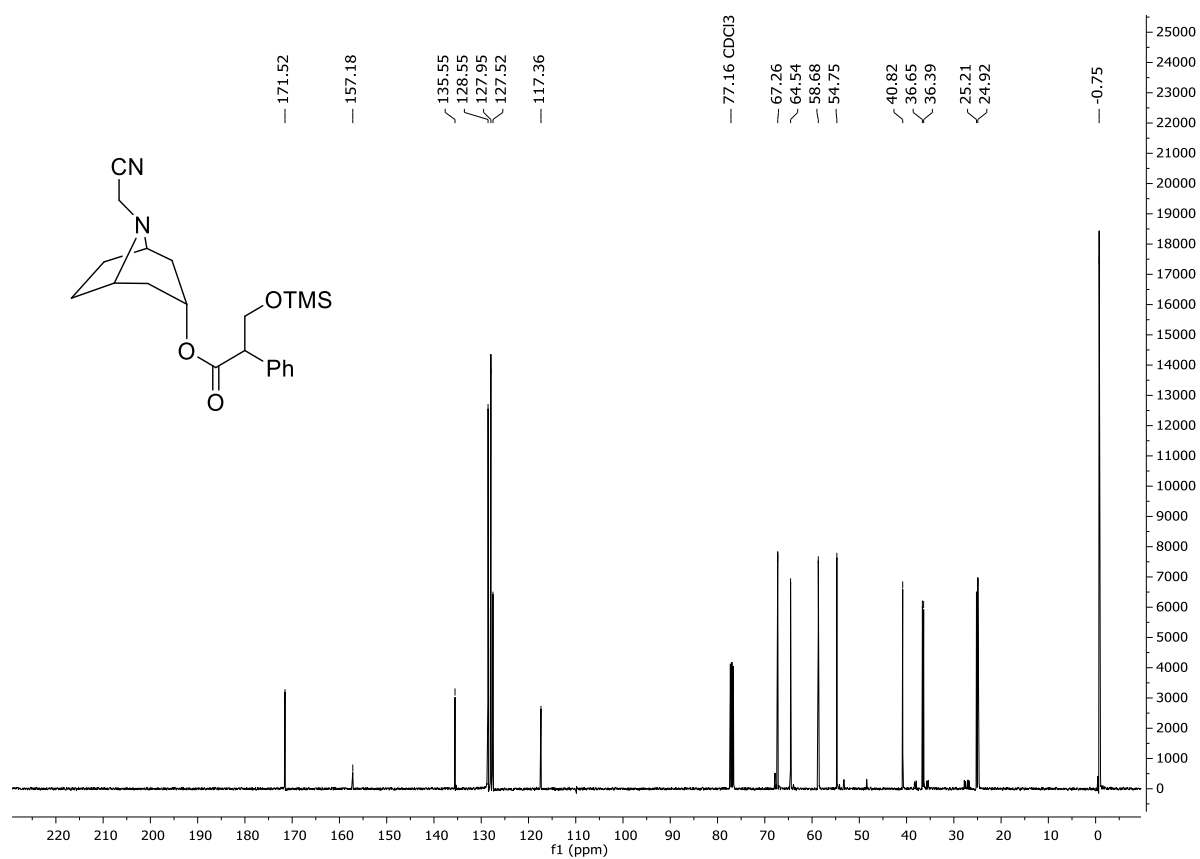


Figure S42. ¹H NMR spectrum (400 MHz, CDCl₃) of 8-(cyanomethyl)-8-azabicyclo[3.2.1]oct-3-yl 2-phenyl-3-[(trimethylsilyl)oxy]propanoate (**21**).

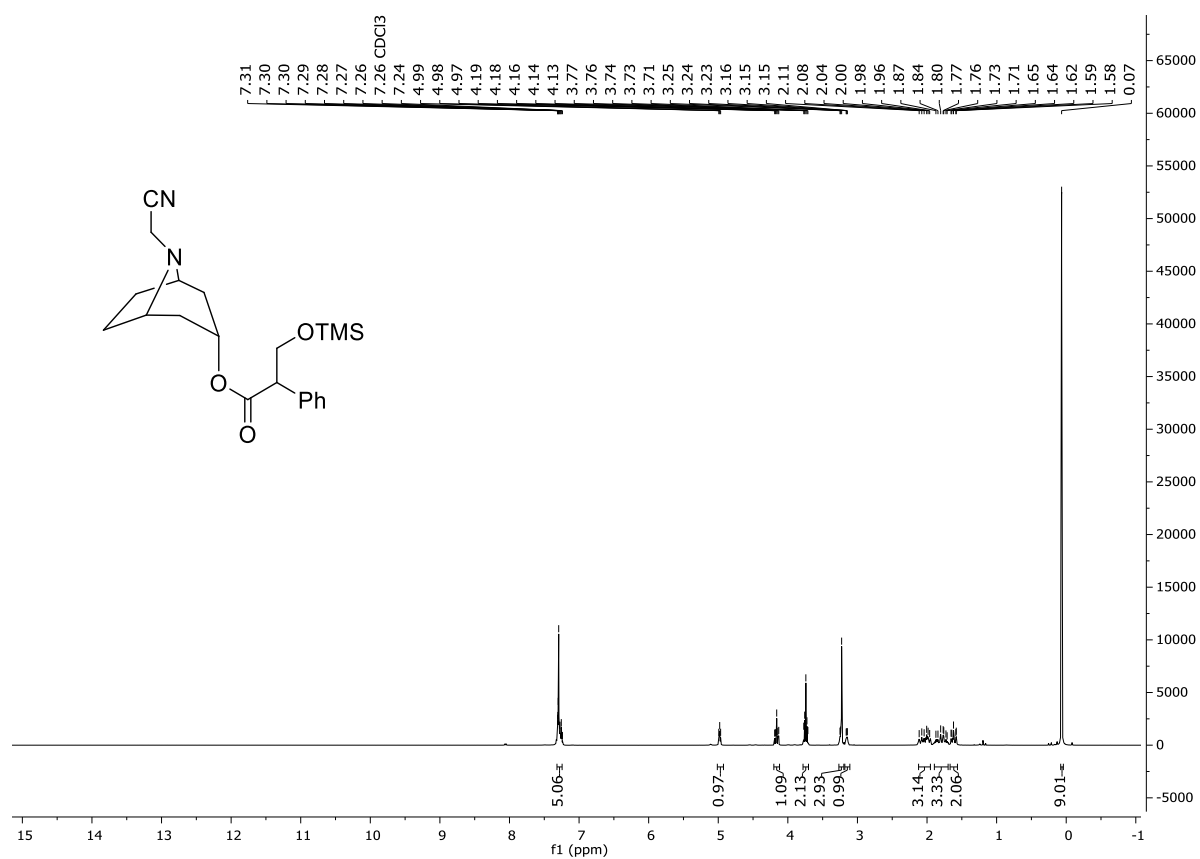


Figure S43. ¹³C NMR spectrum (100 MHz, CDCl₃) of 8-(cyanomethyl)-8-azabicyclo[3.2.1]oct-3-yl 2-phenyl-3-[(trimethylsilyl)oxy]propanoate (**21**).

7. Mechanistic Studies

7.1. ^{29}Si NMR spectroscopic investigation

Reaction conditions: Bu_3N (0.239 mmol, 1.0 eq.) and dry $\text{TiO}_2\text{-DHMIQ}$ (2.5 mg catalyst, 0.6 mol%) were mixed in acetonitrile- d_3 (4.0 mL). The suspension was saturated with oxygen and TMSCN (3.0 eq.) was added. The reaction vial was closed and irradiated with blue light for 3 h. Finally, an aliquot of the irradiated reaction mixture was used for ^{29}Si NMR spectroscopic investigation.

This reaction in deuterated solvent was performed in order to elucidate the fate of the TMS-peroxo species *via* ^{29}Si solution NMR spectroscopy (Figure S44). Four major Si-containing products were identified (Table S6).

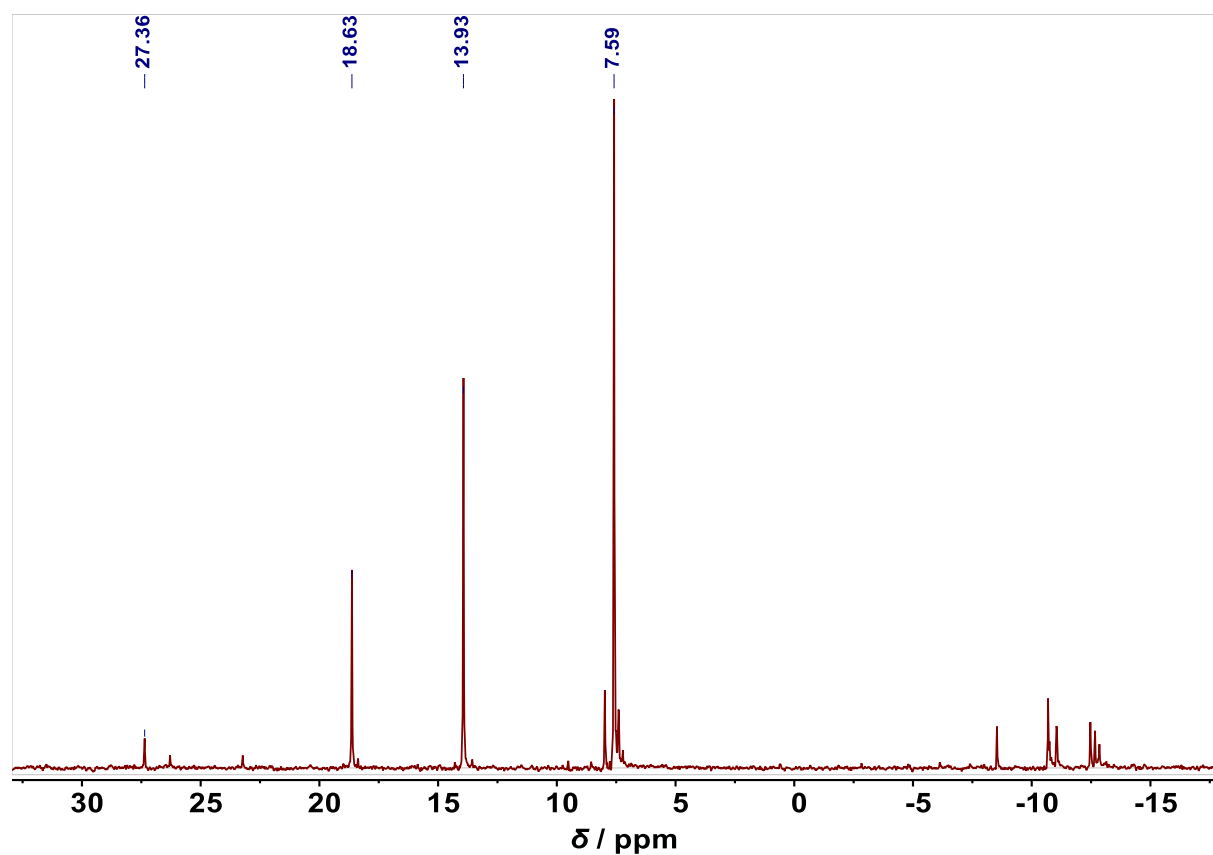
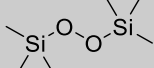
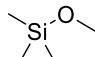
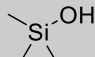
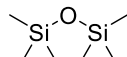


Figure S44. ^{29}Si NMR spectrum (80 MHz, CD_3CN) of a reaction mixture after irradiation.

Table S6. Assignment of ^{29}Si NMR shifts from Figure S44.

Assumed Si species	Found ^{29}Si NMR shift (80 MHz, CD_3CN)	Literature values
Bis(trimethylsilyl) peroxide $\text{Me}_3\text{Si-O-O-SiMe}_3$ 	27.36	27.86 (100 MHz, CDCl_3) ¹⁶ 27.60 (80 MHz, CDCl_3) ¹⁷
Trimethylmethoxysilane $\text{Me}_3\text{Si-OMe}$ 	18.63	18.41 (80 MHz, CD_3CN) ¹⁸ 17.64 (80 MHz, C_6D_6) ¹⁹
Trimethylsilanol $\text{Me}_3\text{Si-OH}$ 	13.93	14.97 (80 MHz, C_6D_6) ²⁰ 12.57 (60 MHz, acetone- d_6) ²¹
Hexamethyldisiloxane $\text{Me}_3\text{Si-O-SiMe}_3$ 	7.59	7.60 (80 MHz, C_6D_6) ²² 7.41 (80 MHz, CD_3CN) ¹⁸

7.2. Control experiments

Screening of alternative pathways

Reaction conditions: Bu₃N (0.239 mmol, 1.0 eq.), dry TiO₂-DHMIQ (2.5 mg) and diethylsilane *or* ethyl acrylate (0.239 mmol, 1.0 eq.) were mixed in acetonitrile (4.0 mL). The suspension was saturated with oxygen and TMSCN (3.0 eq.) was added. The reaction vial was closed and irradiated with blue light for 3 h. The crude product was isolated by extraction and the yield was determined by ¹H NMR spectroscopy with 1,4-bis(trimethylsilyl)benzene as internal standard.

These control experiments were conceived to investigate the possibility of alternative pathways in the reaction mechanism. Apart from our proposed mechanism, α -amino radical intermediates are often discussed in the literature²³ as a mechanistic alternative for iminium formation (Figure S45). The α -amino radical intermediate might be formed in two ways: either by direct H-abstraction from the neutral parent amine (pathway I) or by α -deprotonation of the amine radical cation (pathway II).

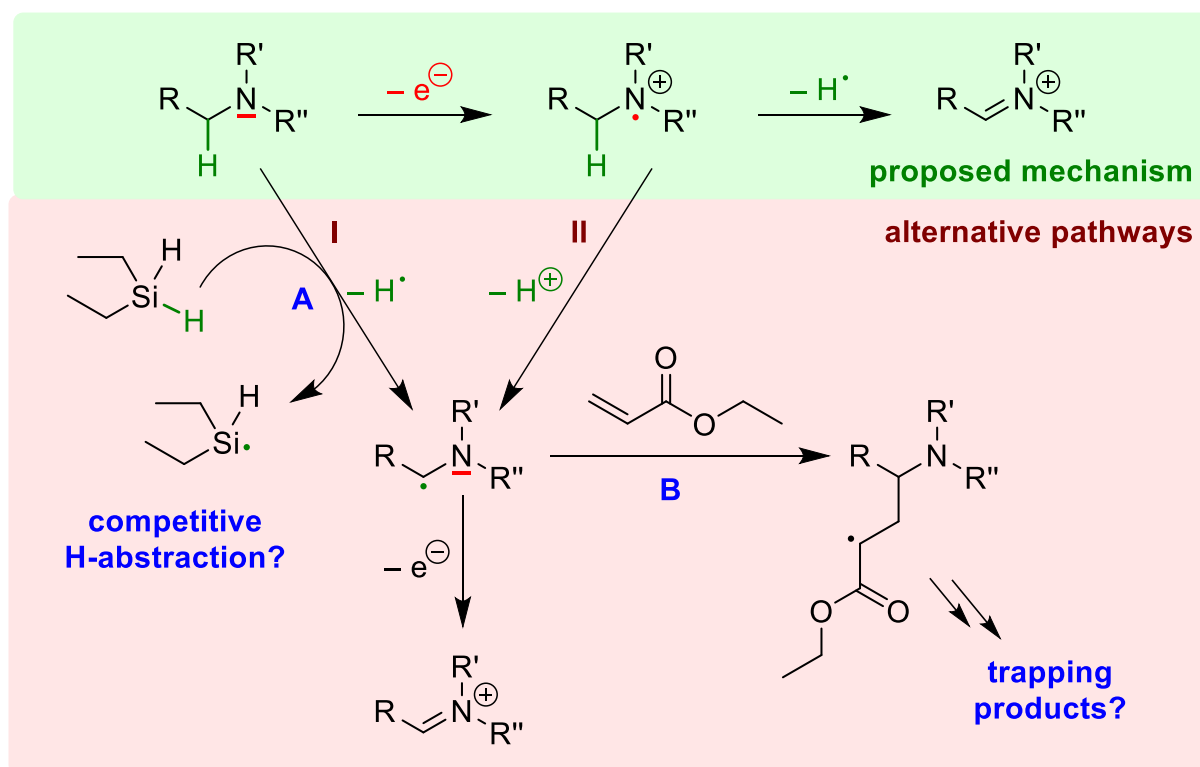


Figure S45. Alternative pathways in the reaction mechanism (pathway I: direct H-abstraction from the neutral parent amine; pathway II: α -deprotonation of the amine radical cation) and applied screening reactions (reaction A: addition of diethylsilane for competitive H-abstraction; reaction B: addition of ethyl acrylate for trapping of α -amino radicals).

To investigate pathway I, we performed a control experiment with addition of equimolar amounts of diethylsilane, whose Si-H bond is slightly weaker than the C α -H-bond of trialkylamines (374 vs. 381 kJ mol⁻¹).^{24,25} If pathway I was the main mechanistic route, addition of diethylsilane would induce competitive H-abstraction, resulting in a reduced yield of the α -aminonitrile product. Since, however, the usual quantitative conversion to the desired product was observed, the presence of diethylsilane does not interfere with the photocyanation of tributylamine. Consequently, the direct H-abstraction from the

neutral parent amine (as described by pathway I) appears less likely and a prior oxidation is suggested which weakens the C α -H-bonds to facilitate the H-abstraction (proposed mechanism).

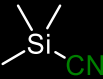
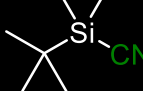
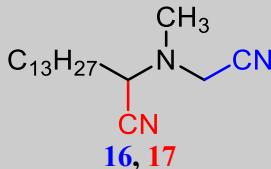
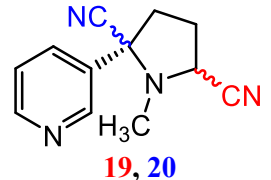
To investigate pathway II as an alternative route for the generation of α -amino radicals, another control experiment was performed with the addition of ethyl acrylate, an electron-deficient olefin which is known to react with α -amino radicals.^{26,27} If α -amino radicals were generated (in any way), addition of ethyl acrylate would produce trapping products which would be easily detectable by NMR. However, no trapping products were observed in this reaction. Instead, the desired photocyanation product was obtained in quantitative yield.

In sum, α -amino radicals appear less likely to be intermediates in the photocyanation reaction. The combined results support the reaction mechanism as proposed in Figure 4.

Reactions with *tert*-butyldimethylsilyl cyanide (TBDMSCN)

Reaction conditions: The photocyanation reactions of *N,N*-dimethyl-tetradecylamine (**8**) and nicotine (**10**) were repeated using the same procedures as described above, with the only exception that the cyanide source TMSCN was replaced with equimolar amounts of TBDMSCN.

Table S7. Regioselectivity for different cyanide sources TMSCN and TBDMSCN.

Cyanated products	TMSCN 	TBDMSCN 
 16, 17	71:29	69:31
 19, 20	56:(28:16)	50:(32:18)

To gain more mechanistic insight into the regioselectivity of the photocyanation, the reactions of *N,N*-dimethyl-tetradecylamine (**8**) and nicotine (**10**) were repeated with the altered silyl species TBDMSCN instead of TMSCN.

The photocyanation reactions with TBDMSCN showed somewhat slower conversion rates, while in both cases, the regioselectivity varied only slightly (Table S7). We interpret this as a result of an accelerating effect of the silylation of hyperoxide which is known to be a less efficient H-abstractor due to its electronic stabilization. With TBDMSCN, the formation of the silylperoxy radical is slowed down due to steric hindrance on Si. We did not expect to see a large difference in regioselectivity as the steric bulk for the H-abstraction changes three atoms away from the reaction center while the nucleophilic substitution at silicon through hyperoxide should be much more affected.

8. References

- (1) Dinh, C.-T.; Nguyen, T.-D.; Kleitz, F.; Do, T.-O. Shape-Controlled Synthesis of Highly Crystalline Titania Nanocrystals. *ACS Nano* **2009**, *3*, 3737–3743.
- (2) Ruchirawat, S.; Chaisupakitsin, M.; Patranuwatana, N.; Cashaw, J. L.; Davis, V. E. A Convenient Synthesis of Simple Tetrahydroisoquinolines. *Synth. Commun.* **1984**, *14*, 1221–1228.
- (3) Katritzky, A. R.; He, H.-Y.; Jiang, R.; Long, Q. 2-Substituted-1,2,3,4-tetrahydroisoquinolines and Chiral 3-Carboxyl Analogues from *N*-Benzotriazolylmethyl-*N*-phenethylamines. *Tetrahedron: Asymmetry* **2001**, *12*, 2427–2434.
- (4) Knabe, J.; Roloff, H. Dehydrierung von tertiären Aminen mit Hg^{II}-ÄDTA, IX. 1-Alkyl-2-methyl-1.2.3.4-tetrahydro-isochinoline. *Chem. Ber.* **1964**, *97*, 3452–3455.
- (5) Janssen, R. H. A. M.; Ch. Lousberg, R. J. J.; Wijkens, P.; Kruk, C.; Theuns, H. G. Assignment of ¹H and ¹³C NMR Resonances of Some Isoquinoline Alkaloids. *Phytochemistry* **1989**, *28*, 2833–2839.
- (6) Wagner, A.; Han, W.; Mayer, P.; Ofial, A. R. Iron-Catalyzed Generation of α -Amino Nitriles from Tertiary Amines. *Adv. Synth. Catal.* **2013**, *355*, 3058–3070.
- (7) Alagiri, K.; Devadig, P.; Prabhu, K. R. Molybdenum Trioxide Catalyzed Oxidative Cross-Dehydrogenative Coupling of Benzylic sp³ C–H Bonds: Synthesis of α -Aminophosphonates under Aerobic Conditions. *Tetrahedron Lett.* **2012**, *53*, 1456–1459.
- (8) Yang, R.; Ruan, Q.; Zhang, B.-Y.; Zheng, Z.-L.; Miao, F.; Zhou, L.; Geng, H.-L. A Class of Promising Acaricidal Tetrahydroisoquinoline Derivatives: Synthesis, Biological Evaluation and Structure-Activity Relationships. *Molecules* **2014**, *19*, 8051–8066.
- (9) Zhang, C.; Liu, C.; Shao, Y.; Bao, X.; Wan, X. Nucleophilic Attack of α -Aminoalkyl Radicals on Carbon–Nitrogen Triple Bonds to Construct α -Amino Nitriles: An Experimental and Computational Study. *Chem. - Eur. J.* **2013**, *19*, 17917–17925.
- (10) Ebden, M. R.; Simpkins, N. S.; Fox, D. N. A. Metallation of Benzylic Amines via Amine-Borane Complexes. *Tetrahedron* **1998**, *54*, 12923–12952.
- (11) Allen, J. M.; Lambert, T. H. Tropylium Ion Mediated α -Cyanation of Amines. *J. Am. Chem. Soc.* **2011**, *133*, 1260–1262.
- (12) Orejarena Pacheco, J. C.; Lipp, A.; Nauth, A. M.; Acke, F.; Dietz, J.-P.; Opatz, T. A Highly Active System for the Metal-Free Aerobic Photocyanation of Tertiary Amines with Visible Light: Application to the Synthesis of Tetraopenerines and Crispine A. *Chem. - Eur. J.* **2016**, *22*, 5409–5415.
- (13) Nauth, A. M.; Otto, N.; Opatz, T. α -Cyanation of Aromatic Tertiary Amines using Ferricyanide as a Non-Toxic Cyanide Source. *Adv. Synth. Catal.* **2015**, *357*, 3424–3428.
- (14) Limousin, G.; Gaudet, J.-P.; Charlet, L.; Szenknect, S.; Barthès, V.; Krimissa, M. Sorption Isotherms: A Review on Physical Bases, Modeling and Measurement. *Appl. Geochemistry* **2007**, *22*, 249–275.
- (15) Firlar, E.; Çınar, S.; Kashyap, S.; Akinc, M.; Prozorov, T. Direct Visualization of the Hydration Layer on Alumina Nanoparticles with the Fluid Cell STEM *in situ*. *Sci. Rep.* **2015**, *5*, 9830.
- (16) Sakamoto, R.; Sakurai, S.; Maruoka, K. Bis(trialkylsilyl) Peroxides as Alkylating Agents in the Copper-Catalyzed Selective Mono-*N*-Alkylation of Primary Amides. *Chem. Commun.* **2017**, *53*, 6484–6487.
- (17) Berchadsky, Y.; Bernard-Henriet, C.; Finet, J.-P.; Lauricella, R.; Marque, S. R. A.; Tordo, P. Persilylated Phosphoranyl Radicals: The First Persistent Noncyclic Phosphoranyl Radicals. *Chem. - Eur. J.* **2006**, *12*, 7084–7094.
- (18) Zhang, Q.; Yuan, H.-Y.; Fukaya, N.; Yasuda, H.; Choi, J.-C. Direct Synthesis of Carbamate from CO₂ Using a Task-Specific Ionic Liquid Catalyst. *Green Chem.* **2017**, *19*, 5614–5624.
- (19) Tsuji, Y.; Taniguchi, M.; Yasuda, T.; Kawamura, T.; Obora, Y. Palladium-Catalyzed Cyanation of Propargylic Carbonates with Trimethylsilyl Cyanide. *Org. Lett.* **2000**, *2*, 2635–2637.
- (20) Ji, P.; Solomon, J. B.; Lin, Z.; Johnson, A.; Jordan, R. F.; Lin, W. Transformation of Metal–Organic Framework Secondary Building Units into Hexanuclear Zr-Alkyl Catalysts for Ethylene Polymerization. *J. Am. Chem. Soc.* **2017**, *139*, 11325–11328.
- (21) Cerkovnik, J.; Tuttle, T.; Kraka, E.; Lendero, N.; Plesničar, B.; Cremer, D. The Ozonation of Silanes and Germanes: An Experimental and Theoretical Investigation. *J. Am. Chem. Soc.* **2006**, *128*, 4090–4100.
- (22) Tobisu, M.; Kita, Y.; Ano, Y.; Chatani, N. Rhodium-Catalyzed Silylation and Intramolecular Arylation of Nitriles via the Silicon-Assisted Cleavage of Carbon–Cyano Bonds. *J. Am. Chem. Soc.* **2008**, *130*, 15982–15989.
- (23) Hu, J.; Wang, J.; Nguyen, T. H.; Zheng, N. The Chemistry of Amine Radical Cations Produced by Visible Light Photoredox Catalysis. *Beilstein J. Org. Chem.* **2013**, *9*, 1977–2001.
- (24) Walsh, R. Thermochemistry. In *The Chemistry of Organic Silicon Compounds*; Patai, S., Rappoport, Z., Eds.; John Wiley & Sons, Ltd: Chichester, UK, 1989; pp 371–391.

- (25) Wayner, D. D. M.; Clark, K. B.; Rauk, A.; Yu, D.; Armstrong, D. A. C–H Bond Dissociation Energies of Alkyl Amines: Radical Structures and Stabilization Energies. *J. Am. Chem. Soc.* **1997**, *119*, 8925–8932.
- (26) Cai, S.; Zhao, X.; Wang, X.; Liu, Q.; Li, Z.; Wang, D. Z. Visible-Light-Promoted C–C Bond Cleavage: Photocatalytic Generation of Iminium Ions and Amino Radicals. *Angew. Chem., Int. Ed.* **2012**, *51*, 8050–8053.
- (27) Kohls, P.; Jadhav, D.; Pandey, G.; Reiser, O. Visible Light Photoredox Catalysis: Generation and Addition of *N*-Aryltetrahydroisoquinoline-Derived α -Amino Radicals to Michael Acceptors. *Org. Lett.* **2012**, *14*, 672–675.